UCLA-ENG-8436
OCTOBER 1984

SEPARATOR PLUGS FOR LIQUID HELIUM

by

Jeffrey M. Lee
S .W.K. Yuan
W.A. Hepler
T.H.K. Frederking

PREPARED FOR THE
NATIONAL AERONAUTICS AND SPACE ADMINISTRATION
AMES RESEARCH CENTER
MOFFETT FIELD, CA 94035

School of Engng.& Appl. Science
University of Calif.,Los Angeles
CA 90024

UCLA-ENG-8436
OCTOBER 1984

SEPARATOR PLUGS FOR LIQUID HELIUM

by

Jeffrey M. Lee
S. W. K. Yuan
W. A. Hepler
T. H. K. Frederking

PREPARED FOR THE
NATIONAL AERONAUTICS AND SPACE ADMINISTRATION
AMES RESEARCH CENTER
MOFFETT FIELD, CA 94035

NOMENCLATURE

A_{tot}	total cross sectional area
D_E	equivalent Ergun diameter
D_p	particle diameter
F(T)	temperature-dependent property function
H_L	bulk liquid enthalpy
H_v	vapor enthalpy
J	total mass flux density
J_o	superficial mass flux density m/A_{tot}
K_p	permeability; (K_{pn} normal fluid value)
K_T	isothermal compressibility
L	length of the porous plug
m	mass flow rate
P	pressure
P_v	saturated vapor pressure
q	heat flux density
Q	total heat flux ; (Q_c heat pumped)
R	radius of curvature
S	entropy per unit mass
T	temperature
v_m	molar volume
V	velocity; (v_{ic} critical value; i = n , s)
w	relative velocity $v_n - v_s$
W	work
z	position coordinate

ε	porosity
η	shear viscosity
λ	latent heat of vaporization
μ	chemical potential
ρ	density
σ	surface tension

SUBSCRIPTS

d	downstream
GM	Gorter-Mellink
n	normal fluid
o	superficial value
s	superfluid
u	upstream
ZNMF	zero net mass flow
λ	lambda transition

TABLE OF CONTENTS

SEPARATOR PLUGS FOR LIQUID HELIUM

J. M. Lee, S. W. K. Yuan, W. A. Hepler, T. H. K. Frederking

I. INTRODUCTION

The present report covers the Summer 1984 research. During conferences in 1984 it has become clear that previously reported results for porous plugs serving as phase separators may be altered significantly by attachment of upstream and downstream devices. An example of the latter is a fluid constriction using a heater. The effort of this Summer 84 has been formulated originally as a set of three tasks:

1. Data analysis

2. Plug measurements

3. Critical assessment of applicability of results

The present report comprises a description of two-fluid-model-related permeability of He II and phase separation in the linear regime (Section II). A brief outline of experiments is given in Section III. Further, a critical discussion is contained in Section IV. Supplement I presents a conference paper dealing with the question of obtaining the Darcy permeability with emphasis on "high" temperature methods. Supplement II is a conference paper on a related topic, i.e. porous plug use for pumping. These supplements are included to give a perspective of "negative" pressure differences, seen from the phase-separator point of view.

II. TWO-COMPONENT EQUATIONS OF THE TWO-FLUID MODEL

The concept of permeability has been a topic of discussion in various fields, such as filtration, chemical engineering-related processes in general, vacuum technology, oilfield reservoirs, bio-systems, and others. In recent time, the advent of advanced space cryogenics support systems for various tasks has added new phenomena at low temperatures (e.g. 1.8 K). The use of

porous media, such as sintered metals, with nominal pore sizes extending from the order of 0.1 to 10 μm has posed several questions. Major transport mechanisms have been clarified in the past few years, however much remains to be done in order to get a comprehensive picture.

The present work continues preceding investigations in the area of space cryogenics related to the task of venting and separating vapor from liquid Helium II. The generally non-Newtonian transport is expressed in terms of the Darcy permeability for Newtonian fluids in the Stokes-Darcy regime. Recent results confirm that "permeability" is indeed useful when the unique definition of the Darcy permeability is kept in mind. Uniqueness requires the limiting value, as the speed goes to zero, and exclusion of Knudsen transport. Further, opening and closing of "dead space" pores is excluded as well.

The emphasis is on the evaluation of various effects which modify the permeability. The two-fluid equations are used. The interdependence of various rates of transport during phase separation is considered. One-dimensional equations are used.

The linear regime of transport is discussed for a vapor-liquid phase separator (VLPS) based on the use of the fountain effect in He II. The thermo-mechanical pressure is directed toward the interior of liquid He^4. The liquid vessel is below the lambda temperature of the He I-He II transition. A low temperature T is on the vapor side and $T+\Delta T$ is on the liquid vessel side. Thus, liquid is kept inside the tank when design conditions are met. Various assumptions underlying a basic system of equations are discussed with subsequent formulations of vector and scalar quantities. The results are inspected in the light of findings reported in the literature, and in the light of experimental evidence.

Device and System Constraints

Consider a phase separator during steady transport of entropy, liquid mass, normal fluid, superfluid, and heat. The five basic statements are the density postulate for the two-fluid system, the mass flux density postulate, the heat flux density, the relative velocity, and the first law constraint for the vapor-liquid interfacial domain at the downstream end of the separator (Fig. 1). Downstream and upstream is viewed from the perspective of mass throughput and heat flow.

Basic two-fluid density postulate. The density of liquid helium is

$$\rho = \rho_s + \rho_n \tag{1}$$

(subscripts n and s denote normal and superfluid respectively). The usual two-fluid approach ignores the condensate fraction referred to in approaches aiming at contact with quantum mechanical parameters (e.g. Ref. 1).

Basic two-fluid flow postulate. After the introduction of postulate (1) it appears to be plausible to assign velocity fields to the two fluids assuming that, at low energy, there exists independent motion to first order: the mass flux density $\vec{J}$ is the sum of two contributions:

$$\vec{J} = \rho\vec{v} = \rho_s\vec{v}_s + \rho_n\vec{v}_n \tag{2}$$

In the formulation of the related quantum hydrodynamics it has been considered useful to introduce a new frame of reference moving with the superfluid velocity v_s. This frame replaces the Euler frame adopted in most cases (e.g. Ref. 2). For instance, the mass flux density (momentum J) is written as $\vec{J} = \rho\vec{v}_s + \vec{J}_o$ (J_o is the J-value in the new frame "K"). The velocity $\vec{v}_s$ of a given liquid element is zero in the frame "K", and the liquid moves with the relative velocity $(\vec{v}_n - \vec{v}_s)$ in "K".

Relative velocity w. In the preceding remarks, the Galilean principle of relative motion has been referred to. Because of the general utility of this type of approach, we employ the relative velocity subsequently:

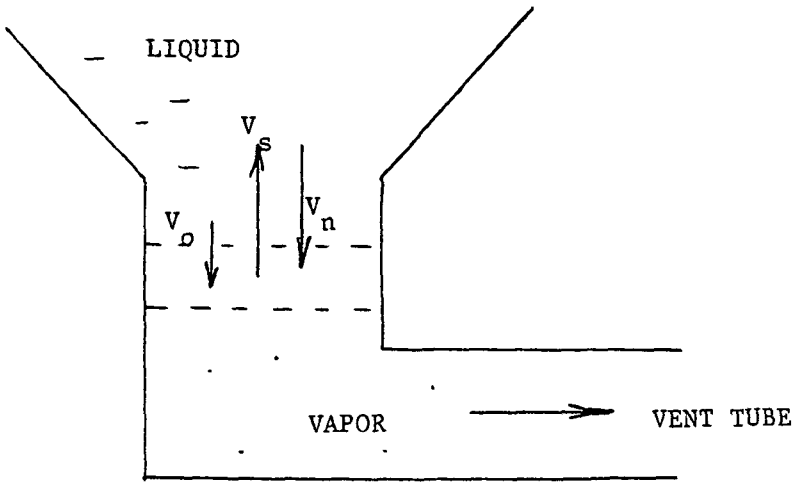

Figure 1. Schematic diagram of porous plug operation in He II in the phase separation regime ;

V_s Superfluid velocity ;

V_n Normal fluid velocity ;

V_o Mass flow velocity .

$$\vec{w} = \vec{v}_n - \vec{v}_s \tag{3}$$

Heat flux density ($\underline{q}$). Original versions of the two-fluid model have been proposed by London and Tisza, and by Landau. Usually, the starting point has been the assignment of entropy to the normal fluid. Thus entropy convection and heat convection is brought about by flow of normal fluid. This leads to the heat convection statement (e.g. Ref. 3). In addition, London[4] formulates $(\rho S) = (\rho_n S_n)$ with S = entropy per unit mass. At very low temperature, T < 0.6 K, phonons are the dominant entropy carriers. The thermodynamics of ideal phonons leads to the results that $(\rho_n/\rho)/(ST) = \text{const} = (\partial\rho/\partial P)_S$ (i.e. reciprocal square of the first sound speed); (P pressure). Thus, we have a limiting value of $\lim_{T\to 0} S_n = \lim_{T\to 0}\left(\frac{\rho}{\rho_n}\right)S = \approx\lim_{T\to 0}\frac{S}{ST} \to \infty$ The normal fluid entropy appears to grow beyond all limits as 0 K is approached. No further use of this relation will be considered subsequently. Instead, in the frame "K", mentioned above, the heat flux density q is expressed as

$$\vec{q} = \rho_s \vec{w} ST \tag{4}$$

First law constraints at the vapor-liquid interface. The first law of thermodynamics for steady flow has been considered frequently. According to the simplest version, the net change of the enthalpy of the flowing streams, across a control volume, bounded by suitable control surfaces, is the sum of the shaft work supplied and the heat transferred. At the ideal interface, no shaft work is made available. Further, per unit area, we have a heat input of q on the liquid side of the interfacial domain (e.g. Ref. 5). Close to the interface the liquid has a low order parameter. Therefore the classical version of the first law is expected to be meaningful. The enthalpy flux entering is $m_L H_L$ while the flux leaving is $m_v H_v$. Thus, the net difference is readily formulated. For steady flow, we have continuity in mass transport, i.e. $\dot{m}_L = \dot{m}_v = \dot{m}$. Therefore, we abbreviate J = mass flux density $(\dot{m}/A)$;

$$\vec{J}(H_v - H_L) = \vec{J}\lambda = \vec{q} \tag{5}$$

The enthalpy difference $(H_v - H_L)$ is the latent heat* of evaporation (λ). Concerning further details of interfacial studies we mention a recent investigation of low pressure evaporation (G. Bertrand and R. Prud'Homme[6]). In addition, H. Wiechert[7] has studied details of the boundary conditions for the liquid-vapor interface of He II. Schotte and Denner[8] introduce kinetics effects arising when the mean free path becomes important, i.e. for the low pressure domain For further information, these references may be consulted.

In summary, the present modeling approach has five basic equations which are useful for a better understanding of the transport processes at least in the linear regime of VLPS systems.

Vector quantities. Consider the five basic equations listed in the preceding discussion. The normal fluid may be eliminated from Eq. (2) using Eq. (3):

$$\vec{J} = \vec{v}_s \rho + \vec{w} \rho_n = \vec{q}/\lambda \tag{6}$$

Elimination of $\vec{w}$ from Eq. (6) by means of Eq. (4) results in

$$\vec{q} = -\vec{v}_s \rho_s ST/[(\rho_n/\rho] - (\rho_s ST/\lambda\rho)] \tag{7}$$

In the vicinity of the lambda temperature (T_λ) we have $\rho_n/\rho \to 1$; $(\rho_s/\rho) << 1$. The expression in brackets on the right hand side of Eq. (7) is positive. It turns out that this is also the case at all T in the roton-dominated range. Thus, the heat flux density $\vec{q}$ is convected in counterflow to the superfluid motion.

The expression $[(\rho_n/\rho) - (\rho_s/\rho)(ST/\lambda)]^{-1}$ is shown in Figure 2 versus T.

* $H_v - H_L = \lambda$ only if ΔT is zero. At the interface the temperature of the vapor and liquid are the same for infinite radius of curvature and high pressures of continuum regimes (we refer also to Appendix C).

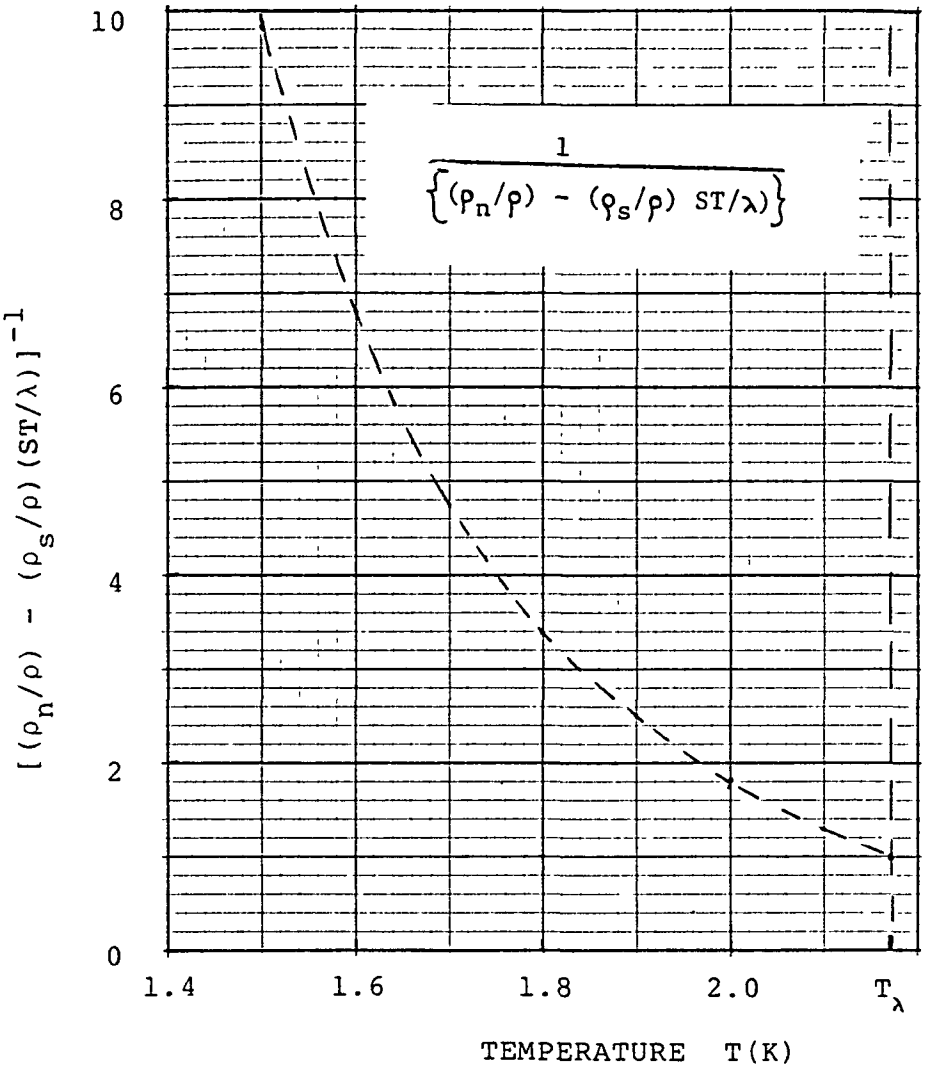

Figure 2. Flow rate factor as a function of the temperature; Equation (7): $\vec{q}/(-\vec{v}_s \rho_s ST)$.

Similarly, the superfluid velocity may be eliminated from Eq. (2) using Eq. (3). The equation for j is written now as

$$\vec{j} = \rho\vec{v}_n - \rho_s\vec{w} \tag{8}$$

Again, the relative velocity is eliminated using Eq. (4):

$$\vec{q} = +\rho\vec{v}_n ST\lambda/(\lambda+ST) \tag{9}$$

The expression in the denominator of the right hand side of Eq. (9) is positive. Thus, $\vec{q}$ is in the direction of $\vec{v}_n$, in agreement with normal fluid behavior postulated for the two-fluid system. According to eq. (9) one may write

$$\vec{q} = \vec{q}_{ZNMF}(1 + ST/\lambda)^{-1} \tag{10}$$

The reference quantity is the zero net mass flow rate $\vec{q}_{ZNMF}$. As T is lowered sufficiently, ST becomes much smaller than the latent heat. Therefore, the solution for zero net mass flow is approached asymptotically, as discussed elsewhere[9]. Details of the preceding treatment are in Appendix A.

Mean transport rates and mean speeds. The special flow constraints of the zero net mass flow (ZNMF) mode are rather well known. There appears to be no rigorous local condition derived from Eq. (2) for $j = 0$. In other words, the flow fields of Newtonian-like normal fluid flow with a parabolic velocity distribution, and those of the superflow with a "plug flow" distribution permit satisfaction of $j = 0$ only at one particular location of pipe flow. However, mean values of the flow equation do satisfy the scalar equation $|\overline{j_s}| = |\overline{j_n}|$, or

$$|\overline{j_s}| = \rho_s|\overline{v_s}| = \rho_n|\overline{v_n}| = |\overline{j_n}| \qquad \text{(ZNMF)} \tag{11}$$

Figure 3 represents examples of vectors compatible with Eq. (2) (case (a) is a possibility which might be realized in a porous plug; case (b) is the parallel vector arrangement). The inset of Figure 2 presents the parallel case for the relative velocity (w), the superfluid velocity and the mass flux

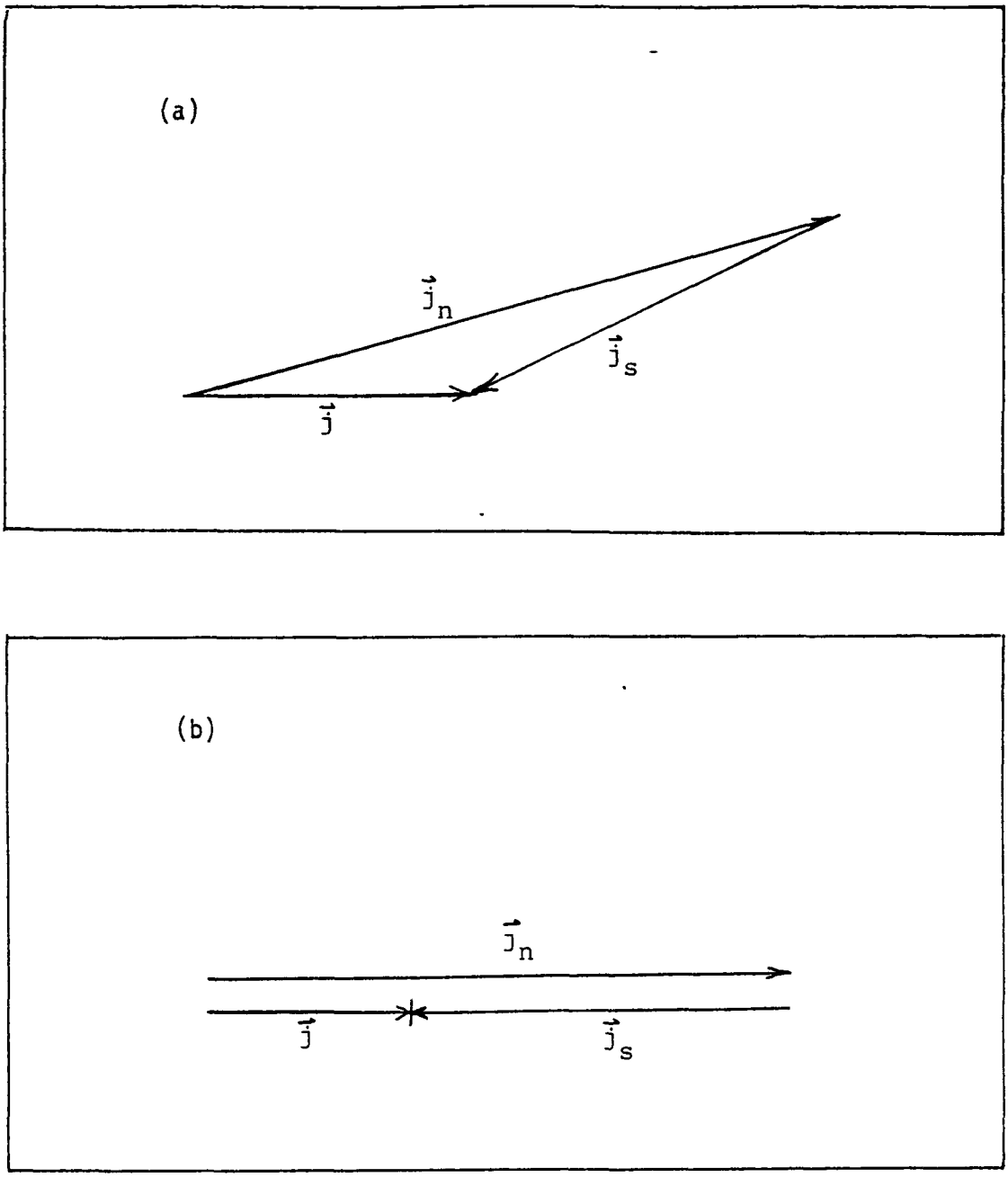

Figure 3. Examples of vectors of the two-fluid model description of vapor-liquid phase separation;
a. Different directions of superfluid velocity,normal fluid velocity and mass flow velocity ;
b. Parallel velocities .

density j.

The mean heat flux density of Eq. (10) is written as

$$|\overline{q}| = +\rho_s|\overline{v_s}|ST/[(\rho_n/\rho) - (\rho_s/\rho)(ST/\lambda)] \qquad (12)$$

Some additional details are given in Appendix B.

Van Sciver[10] has presented an interpretation of the transport phenomena resulting from a superposition of a transport velocity on the specific case of Gorter-Mellink counterflow. The underlying equation is deduced from an adoption of an Euler coordinate frame. Thus, the usual thermal energy equation is replaced by

$$\rho\, DH/Dt \equiv \rho[\partial H/\partial t + v\partial H/\partial x] = -\partial q_{GM}/\partial x \qquad (13)$$

$[q_{GML} = -f(T)(\partial T/\partial x)^{1/3}]$ is the Gorter-Mellink equation for the counterflow heat flux density; f(T) is the Gorter-Mellink temperature functional; H is enthalpy. For steady flow we have $\partial H/\partial t = 0$. The preceding one-dimensional equation for flow along the x-direction becomes

$$dH/dx = +f(T)d(dT/dx)^{1/3}/dx \; ; \quad \Delta T << T \qquad (14)$$

The previous transport equation of the two-fluid approach is not entirely consistent with the special equation (14). Once consistency with Van Sciver's approach is incorporated, the preceding equation for q (Eq.10) is to be replaced by

$$q = q_{ZNMF}(1 - ST/\lambda)^{-1} \qquad (15)$$

The factor $(1-ST/\lambda)^{-1}$ is displayed in Figure 4 versus the temperature. The two-fluid result, Eq. (10), is included. The difference between the two-fluid mode Eq. (10) and Eq. (15) is about 23% at 2.1 K.

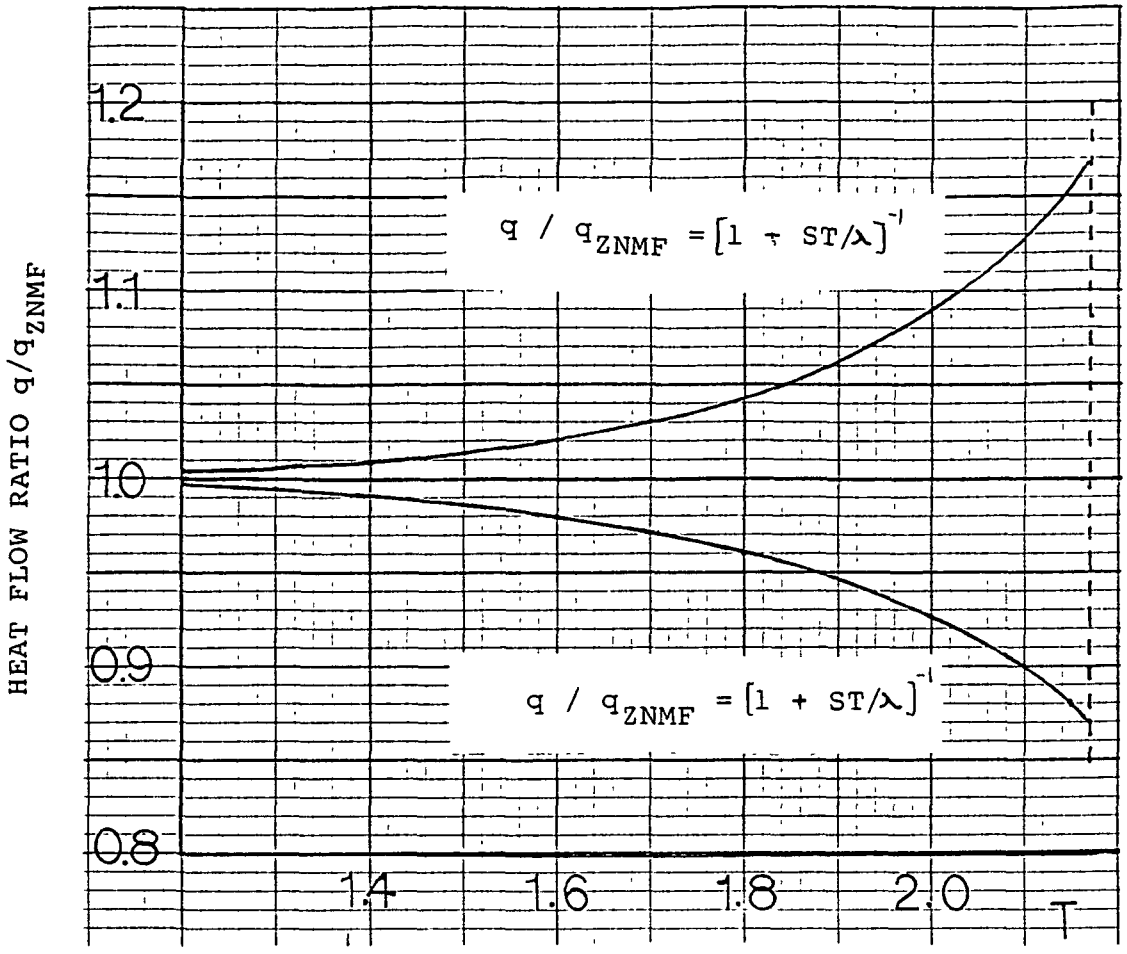

Figure 4. Heat flow ratio of q/q_{ZNMF} as a function of the temperature.

Discussion of T-influence and related work. In general the superposition of mass flow and heat flow may be arranged independently by external means. For the special geometry of transport through a duct with adiabatic walls one may distinguish the two cases of $\vec{q}$ and $\vec{j}$ in parallel, and $\vec{q}$ and $\vec{j}$ in counterflow. In the VLPS system however, the first law constraint (Eq. 5) couples the two transport rates of heat and mass. Thus, $\vec{q}$ and $\vec{j}$ are kept in parallel. The analysis of Van Sciver[10] has been based on the turbulent flow studies of Johnson and Jones. For the parallel case there is an enhancement of q beyond the ZNMF value. In contrast, the two-fluid model Eq. (10) predicts a lowering of q with respect to the ZNMF mode.

It is noted that the idealized vapor-liquid interface may have a less ideal domain than presumed in the linear system of equations. This is expected when turbulence and/or vibrations start to shake the interface. However, "classical" findings on evaporation in the presence and absence of monolayers have resulted in the conclusion that pure heat conduction in the interface-adjacent layer is the dominant mechanism (G. T. Barnes and D. S. Hunter[11]). Thus, for a certain class of VLPS phenomena, a similar restriction related to He I-like diffusion is expected to dominate the liquid layer of low order parameter close to the vapor. Concerning details of the microscopics, we refer also to the review of R. Evans[12] on "The Nature of the Liquid-Vapor Interface". The He II-vapor interface has been treated by Hills et al. in another paper[13].

The temperature difference due to surface tension is outlined in Appendix C. The one-dimensional analysis of the non-linear transport regime by van Sciver is sketched in Figure 5 versus the flow parameter used in Ref. 10. When the entropy and mass flow rates are in parallel as for the VLPS mode, the heat transport rate is increased. It is noted that this increase in the data range documented by Johnson and Jones[14] does not exceed a factor of 2. As discussed previously, the vapor-liquid phase separator has entropy flow in parallel with mass flow.

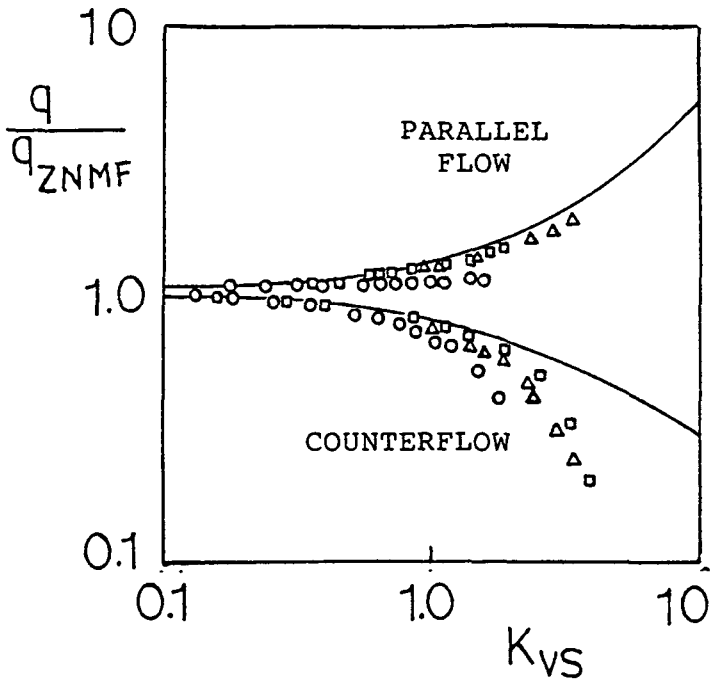

Figure 5. Heat flux ratio vs. flow parameter K_{VS} of Van Sciver (ref. 10); K_{VS} is proportional to the thermal energy convection rate of forced flow with speed v to the Gorter-Mellink convection rate.

Another example of indirect evidence supporting a lowering of the heat transport rate during counterflow of entropy and mass has been presented by Tough and Baehr[15]. Critical conditions have been considered. Further, it is noted that attention is on the duct downstream of a pump and not on the porous medium. A fountain effect pump is used. It causes flow of liquids in counterflow with the normal fluid flow in the porous medium. At critical conditions, characterized by the subscript c, upon an increase of $|v_{nc}|$, the flow rate expressed as $|v_c|$ is decreased. Thus, there is partial confirmation of the consequences of the Van Sciver approach for the critical conditions of the two-fluid system. The results of Tough and Baehr[15] are given for 1.4 K and 1.6 K. The data are contained in Figure 6.

III. EXPERIMENTS

The apparatus used has been similar to the one described previously[16]. The change incorporated in the present setup has been the elimination of the flow modulator studied previously. An outer liquid Helium II bath surrounds a central vent tube with a porous plug located at the lower end of the vent tube. Vent conditions are modified by a set of two valves (bypass and butterfly valve).

Procedures are identical as far as the general preparation is concerned. During the tests, various positions of the valves have been used to cause different vapor flow impedances. The range of flow is varied in a finite mass flow rate interval caused by heat supply to a heater located in the "bath". The bath proper is a jacket surrounding the central tube. The jacket in turn is immersed in the outer bath. The liquid level in the jacket is a monotonically decreasing function of time during the tests caused by the heat supply. After several runs the liquid level becomes too low. Once this state has been reached an outer "thermo-pump" is activated by heat supply at the downstream end of the pump. The liquid is transferred into the jacket by this pump using the fountain effect, as described in Supplement II.

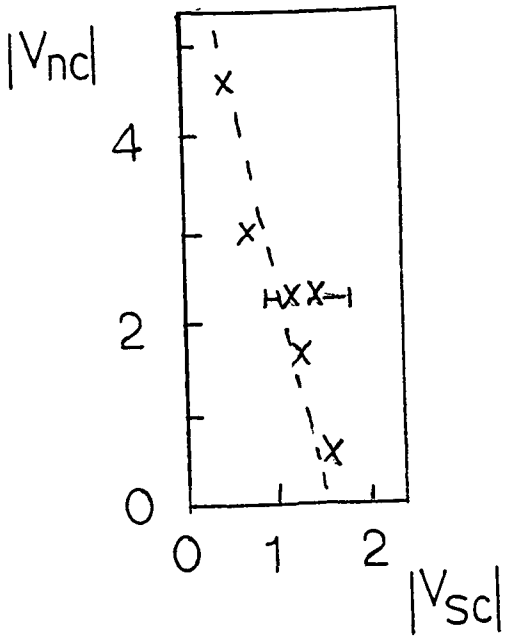

Figure 6. Results for counterflow of mass and entropy in a porous medium for critical conditions (Tough-Baehr[15]).

Note: Tough and Baehr place emphasis on a duct attached to the pump using negative flow velocity as sign convention for this duct.

The resulting flow rates deduced from level changes are affected by gross unbalances in heat supply, bath temperature, and valve position. By varying valve cross sections available, in order to match the heat supply rate, a certain "bath" temperature interval is covered rather close to quasi-steady conditions. (If this is not the case the bath temperature either drifts down or increases upwards). Data taken are affected by the degree of stability created by the valve impedance selected. The ideal case of constant mass flow rate is enforced when there is a large impedance. However this case is characterized by rather small throughput of mass through the plug. Therefore, a number of runs are established at conditions farther away from the constant mass flow case. This is necessary in order to cover a reasonable mass flow range in one set of experiments.

Figure 7 shows Darcy permeability results for various plugs at room temperature. D_E is the equivalent Ergun diameter. This diameter has been modified using the porosity ε. The throughput length L_C is the square root of the Darcy permeability. If there exists a packing geometry exactly equivalent to a spherical particle system rather closely packed, the diameter D_E is expected to vary but little. The actual data spread indicates a finite spectral range associated with the particular plug system under consideration. Details of the underlying concepts are given in Supplement I.

Experimentally obtained quantities are displayed in the next Figures 8 through 13. The variables are shown versus the time t as obtained during the experimental runs.

Figure 8 presents the decrease of the liquid level z with time t. From the conservation of mass condition, velocities and thermal energy convection rates through the porous plug are calculated. The mean velocity is displayed in Figure 9. The heat flux $\dot{Q}$ is obtained from the first law constraint at the plug exit (Figure 10).

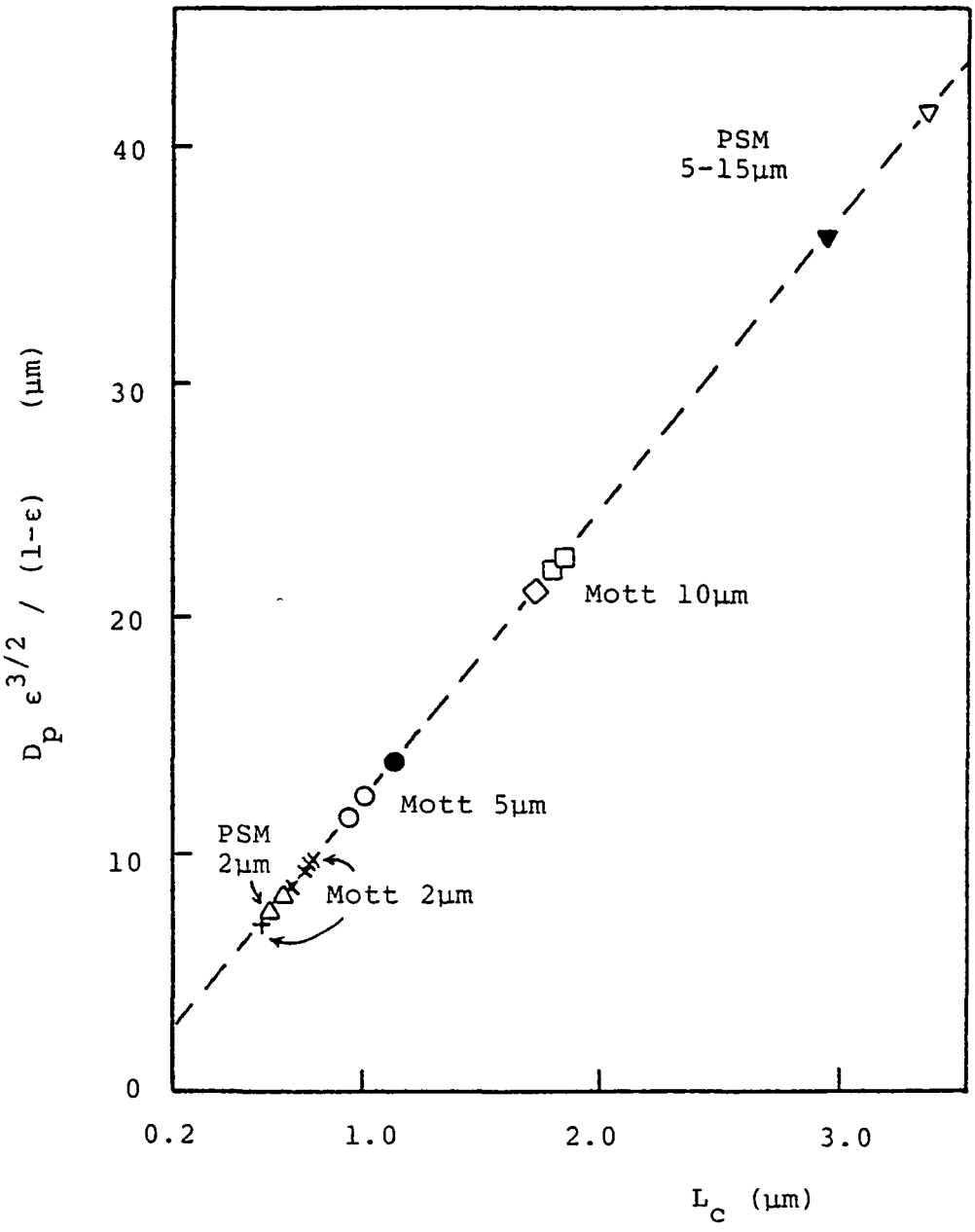

Figure 7. Distribution of the porous plugs classified by the Darcy characteristic length.

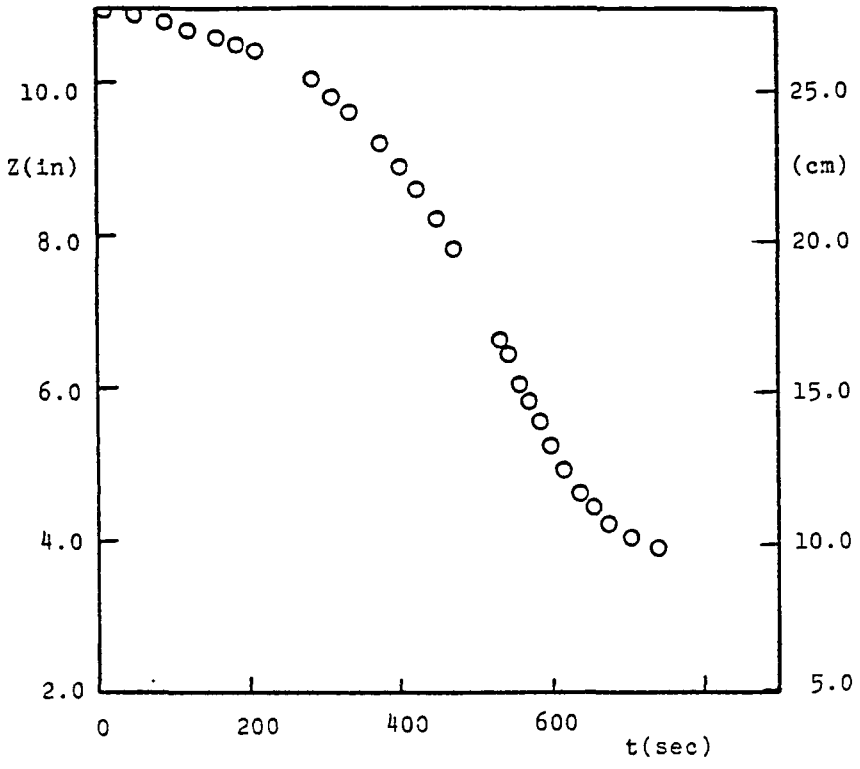

Figure 8. Liquid level change with time during VLPS run;
(Plug : Bronze; nominal pore size 5 - 15 μm);
(This plug has been used in the various runs
for which data are shown in subsequent figures).

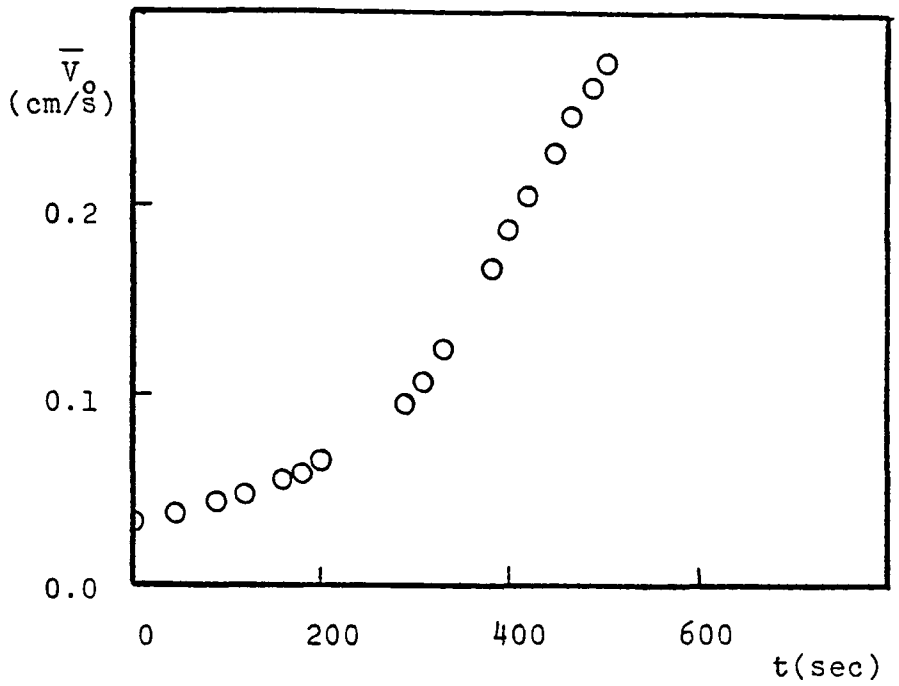

Figure 9. Mean flow velocity (superficial value) of mass flow through the plug

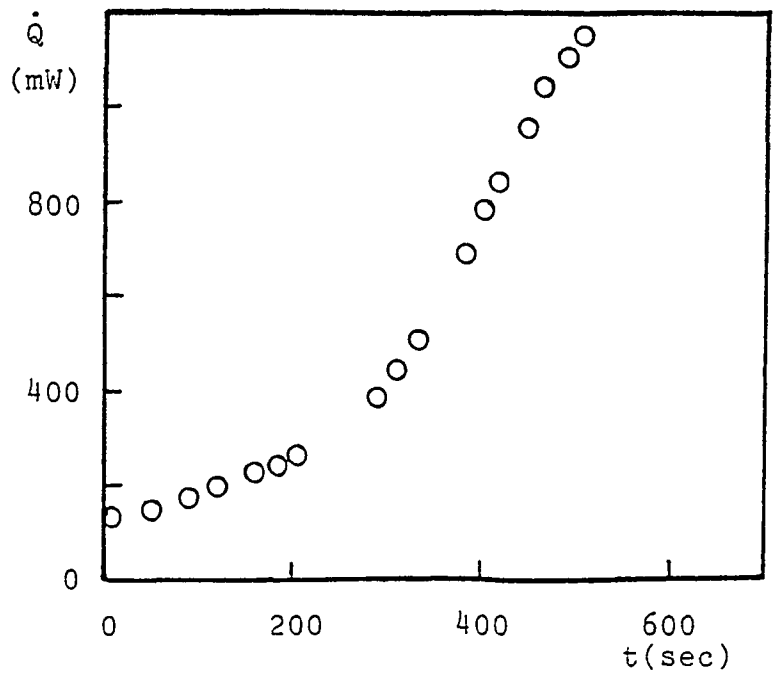

Figure 10. Heat flux rejected during transport through the plug

The bath temperature change during slow changes of state is plotted as a function of time in Figure 11. The bath temperature is the upstream temperature T_u of the plug. Figure 12 shows the temperature difference across the plug. Figure 13 presents the pressure difference obtained from the pressure transducer readings.

Once steady transport or quasi-steady conditions are secured, the "effective permeability" is readily available. In general, the data are in the non-linear regime for the plug results of the preceding Figures 8 through 13.

The mass flow rate $\dot{m}$ expressed as $\vec{v}_o$ is shown in Figure 14 for three different bath temperatures of 1.55 K, 1.6 K and 1.85 K.

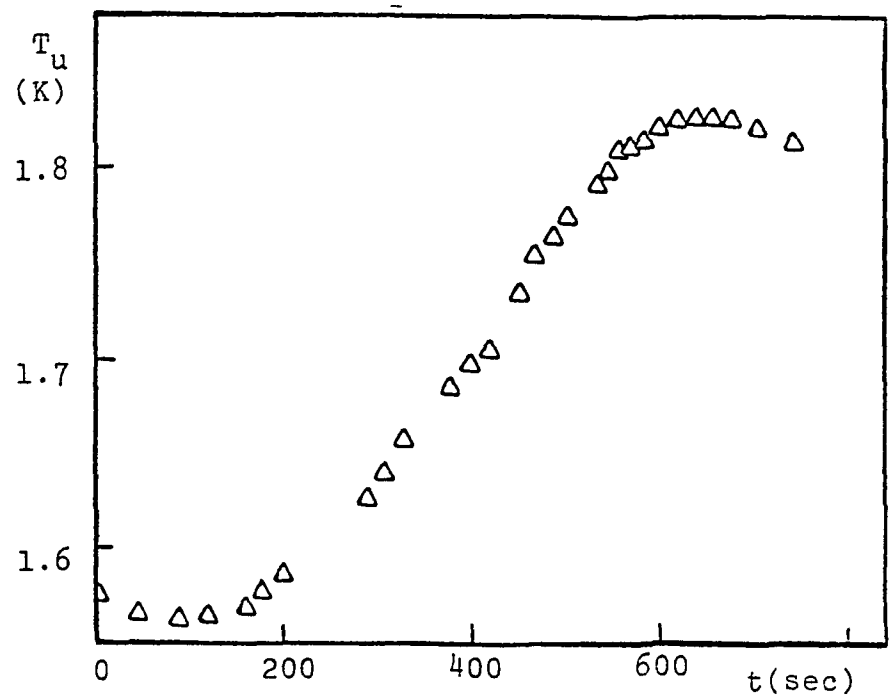

Figure 11. Bath temperature T_u as a function of time

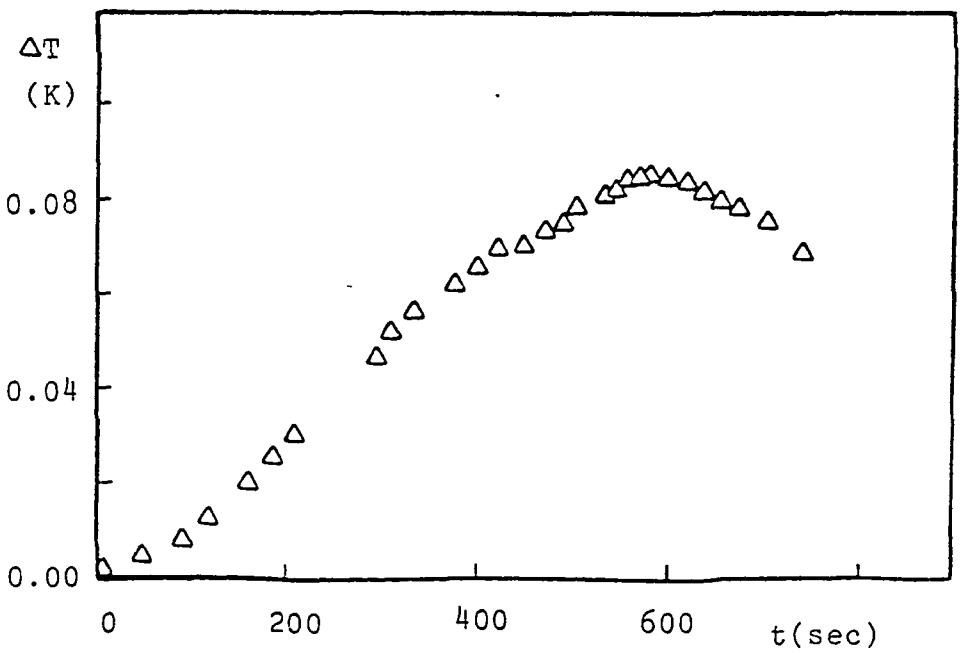

Figure 12. Temperature difference across the plug

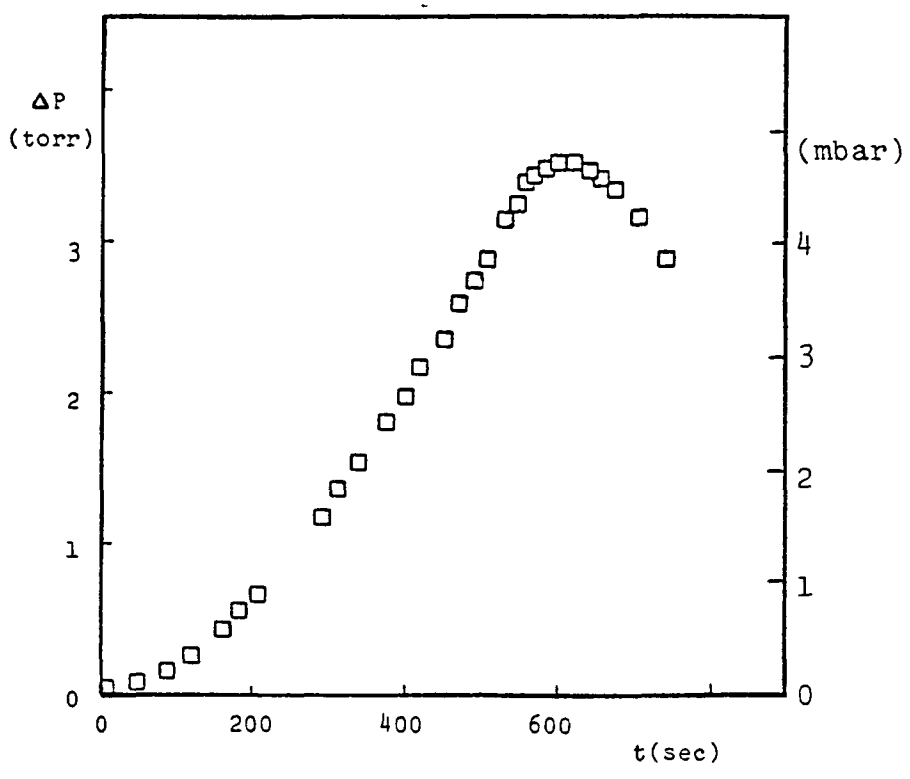

Figure 13. Pressure difference across the plug

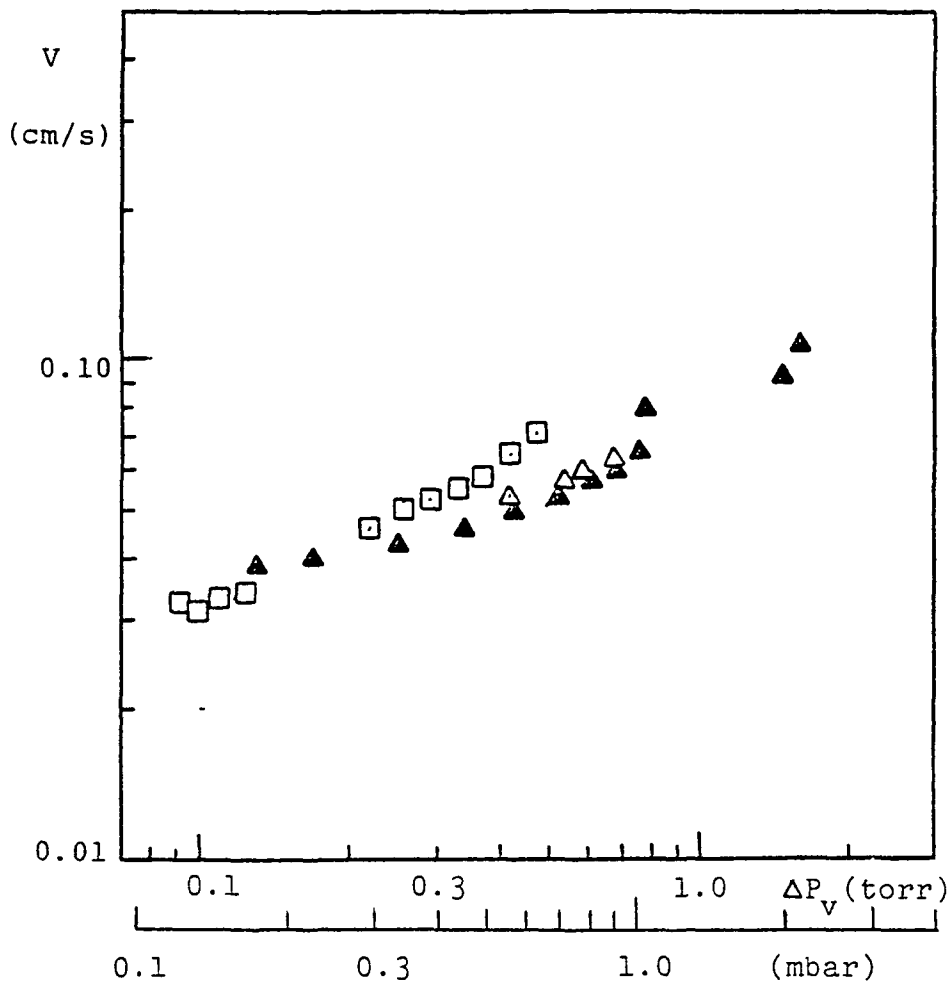

Figure 14. Velocity versus vapor pressure difference at various temperatures.

IV. DISCUSSION AND CONCLUSIONS

The present set of equations may be used to find the mass flow rate $\dot{m}$ versus the pressure difference ΔP_v in the linear regime of the porous plug phase separator. In the analysis only a few equations are needed to obtain the mass flow rate from an integration. The following equations are used for steady transport at relatively large ΔT and ΔP_v respectively:

1. Coupling condition for entropy and mass flow.

2. Mean normal fluid convection rate as a function of the driving temperature gradient.

3. Ratio of mean q_o-value of the porous medium to the mean q_o of zero net mass flow.

4. Mass flow rate as integral of a T-dependent function F(T) (presented below).

5. Vapor pressure function (T-58) for conversion from ΔT to ΔP_v.

The preceding set leads to the mass flow rate of steady transport in terms of thermophysical properties:

$$\dot{m} = K_{pn}(A_{tot}/L) \int_{T}^{T_\lambda} F(T)dT \tag{16}$$

K_{pn} is the normal fluid permeability (Darcy law analog in the linear regime). A_{tot} is the total plug cross section. L is the axial length, i.e. the depth of the plug. The property integral is written as follows:

$$F(T) = \rho^2 S^2 T(1-ST/\lambda)^{-1} \eta_n^{-1} \lambda^{-1} \tag{17}$$

(ρ liquid density, λ latent heat of vaporization, η_n shear viscosity of the normal fluid).

Figure 15 shows the ratio of $(\dot{m}/K_{pn})$ as a function of temperature when the T-range covered extends from a bath temperature of T all the way to the lambda temperature T_λ. For any other interval (T_2-T_1), the mass flow rate may be determined using the difference function

$$\left[\dot{m}/K_{pn}\right]_{T_1}^{T_\lambda} - \left[\dot{m}/K_{p}\right]_{T_2}^{T_\lambda} = \left[\dot{m}/K_{pn}\right]_{T_1}^{T_2} \qquad (18)$$

Figure 16 presents $(\dot{m}/K_{pn})$ as a function of the vapor pressure difference ΔP_v. The function is qualitatively similar to Equation (16). In both Figures 15 and 16 a ratio (A_{tot}/L) of unit length has been introduced for simplification.

Use of the thermophysical property integral for an arbitrary transport case usually leads to a non-linear K_{pn}-function. In experiments, however, this may also indicate that the linear regime was not established over the entire length of the plug. A VLPS example is shown in Figure 17. The K_{pn}-value obtained at the lowest temperature is much closer to the Darcy analog value than at any other temperature. The data constitute "effective normal fluid permeabilities". It is noted that the (dashed) reference value is for a similar plug (1 μm nominal pore size, material: aluminum silicate). (Further details are given in Supplement I.) The phase separation process is quite close to the ZNMF mode. Therefore another comparison is useful for understanding of porous media observations.

Figure 18 is a data set for the ZNMF mode of the early pioneering work of Allen and Reekie[17]. This particular result has been reproduced in the book by W. H. Keesom, Liquid Helium[18]. A powder-filled tube had been used by Allen and Reekie. Therefore, this set of data appears to be among the earliest porous media results for He II. The original figure of these authors (Fig. 2 of Ref. 17) appeared to have been a matter of considerable discussion because of the use of the "total conductivity" of the packed bed, given as "(watts/K,sec)". Professor Allen kindly responded to an inquiry about this point with letter of June 25, 1984. He notes that "it is hard to recall the precise way in which the measurements were made in the paper with the late Jim

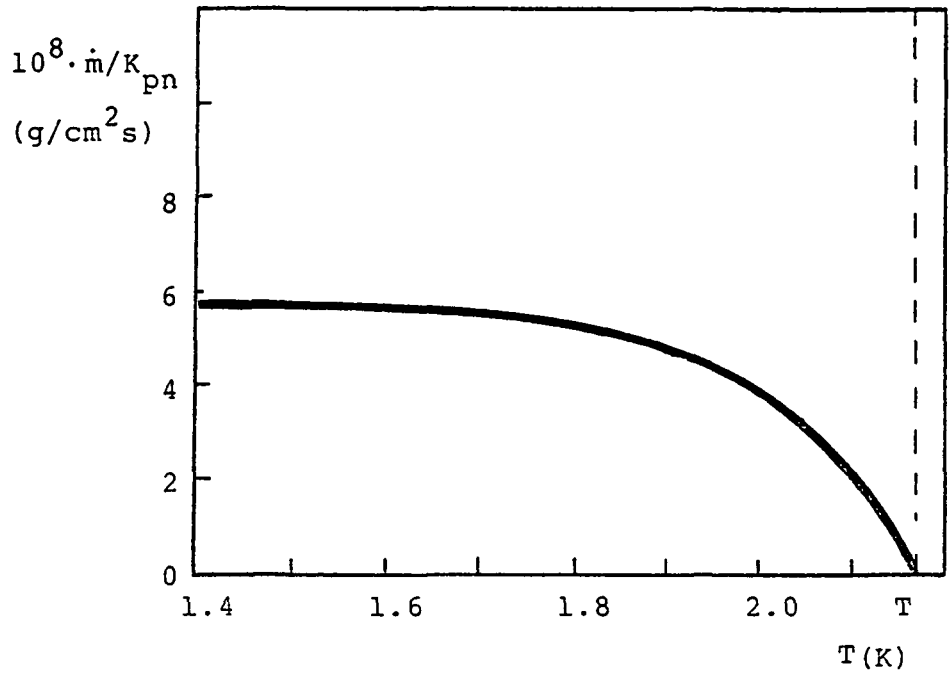

Figure 15. Normalized flow rate to permeability ratio for (A_{tot}/L) of unit length (1 cm).

Integral for T-range from T to the lambda temperature is plotted as value at the low initial temperature on the downstream end of the plug.
Numerical values have been selected in order to compare with ref.20 (1μm plug).

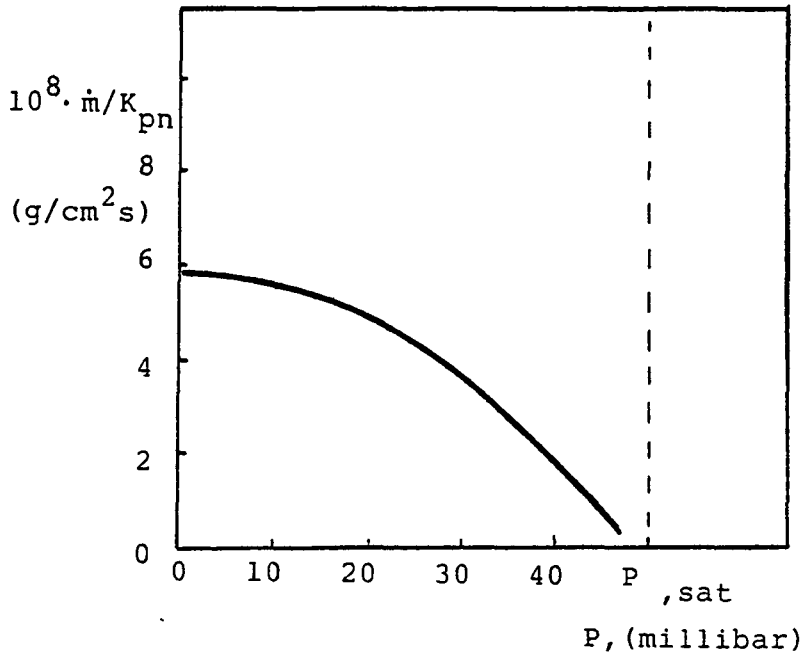

Figure 16. Normalized mass flow rate to permeability ratio of Fig. 14 vs. pressure;

The integral all the way from the downstream state to the lambda point (saturated liquid) is plotted at the downstream value of P.
Numerical values have been selected in order to compare to ref. 20 (1μm plug).

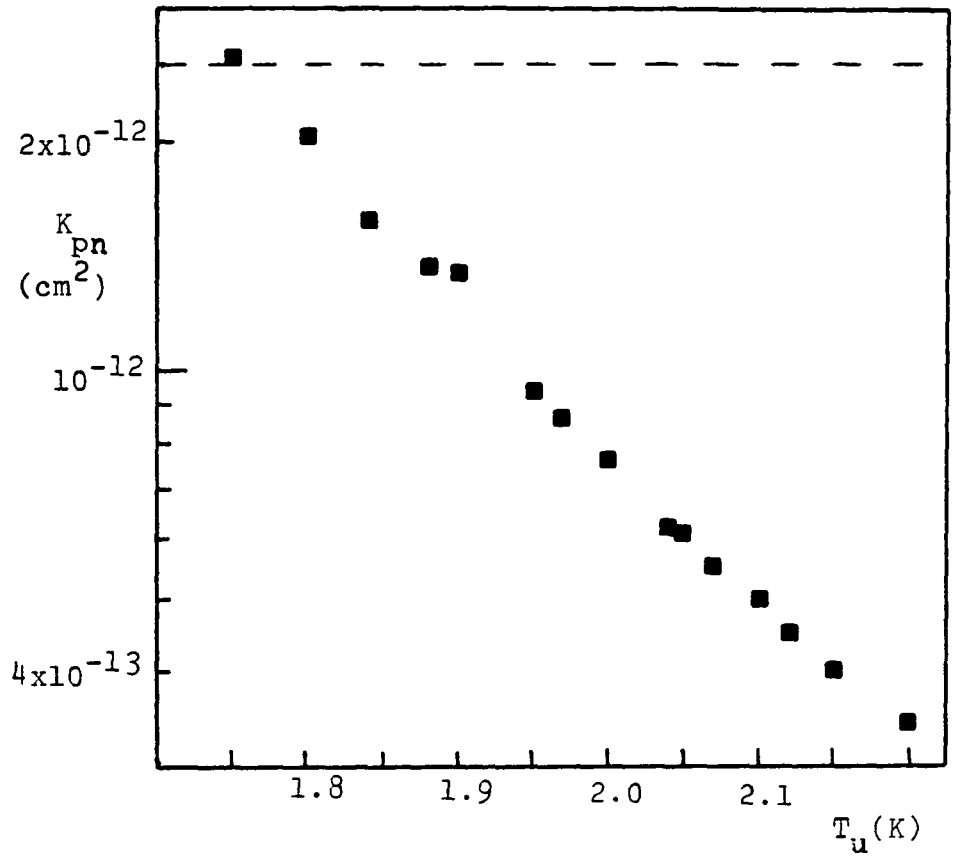

Figure 17. Effective permeability K_{pn} of flow through 1 μm plug (norminal size, of Klipping group (20) ;) (Evaluated: Courtesy: Chau Nguyen):

Note: the data trends are reminiscent of the early results of Allen-Reekie (ref. 17) in the non-linear regime (Figure 18).

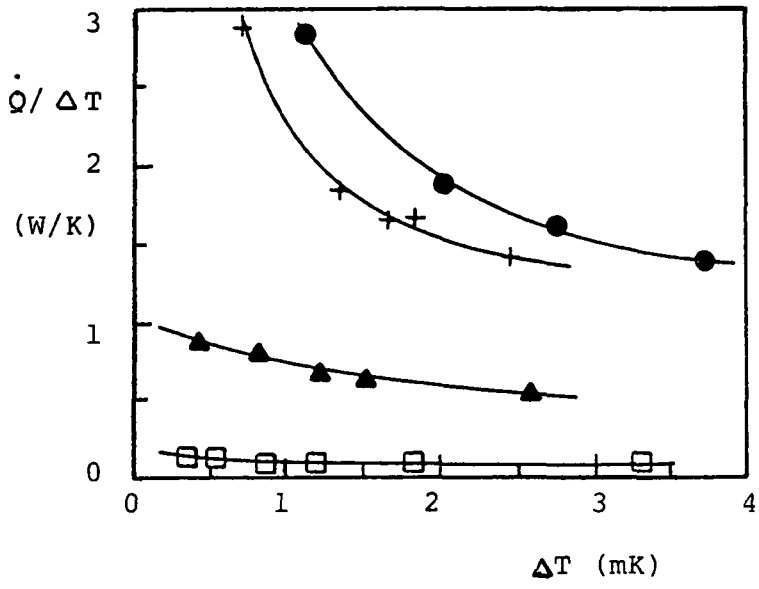

Figure 18. Data of Allen-Reekie[17]; total conductance versus temperature.

(powder-filled tube, particle size, 100 μm ~ 500 μm)

Courtesy of J.M. Lee (ref. 21)

Reekie, especially as my old note books do not seem to have survived. However, re-reading the description of the measurements of Figure 2, I think the best description is in the first three lines at the top of p. 118, which refers to Figure 1(b). It was the wattage put into the heater H divided by the rise in temperature at the thermometer T when equilibrium was reached. T had been calibrated against the vapor pressure, and this was also measured when equilibrium was reached. As far as I recall, we did not have a second resistance thermometer in the bath, but we did have a good cathetometer."

Therefore, the letter indicates rather convincingly that the units might have been "watt-sec/(K sec)", i.e. the thermal conductance $[\dot{Q}/\Delta T]$ is given as [W/K]. The Allen-Reekie result in Figure 18 has been reproduced in this form as $\dot{Q}/\Delta T = A_{tot}\vec{q}_o/\Delta T$. At high values $[\dot{Q}/\Delta T]$ at 1.9 K there is a very non-linear behavior. At the lowest bath temperature however the data appear to produce a nearly constant conductance. In other words, the data are close to the limit of K_{pn} = const.

Conclusions. The following conclusions are suggested from the present Summer.1984 studies:

1. The VLPS results appear to be indeed close to zero net mass flow in agreement with theoretical prediction.

2. There is a small enhancement of the heat flux density $\vec{q}_o$ with respect to the zero net mass flow mode predicted by the Van Sciver model. Experimentally this enhancement seems to be masked by other secondary effects.

3. The results obtained with several plugs appear to be consistent with zero net mass flow in so far as there are considerable departures from the linear regime prediction. This is confirmed for the present plug in the pore size order range of 10 μm (nominal value).

4. The normal fluid analog of the Darcy permeability is usually an "effective" value outside the linear regime. Procedures to come close to the Darcy analog case are most successful for large pores when the

temperature is lowered and when ΔT is decreased.

ACKNOWLEDGMENTS. We are most grateful for the help of Romeo Carandang, Tuan Anh Le, Chau T. Nguyen*, and Cathy Arboleda during experiments, in data reduction and in theoretical calculations. These collaborators did an extremely laudable job without being compensated for it during the period of work. The efforts of this select volunteer group are very much appreciated.

*) Present address: Rockwell International.

V. REFERENCES

1. C. Linnet et al., Adv. Cryog. Eng. 19, 1974, 365.

2. I. M. Khalatnikov, Introduction to the Theory of Superfluidity, Benjamin, New York, 1965.

3. F. London, Superfluids, Vol. 2, Wiley, New York, p. 78.

4. F. London, op. cit., p. 61.

5. Y. I. Kim et al., Rept. UCLA-ENG-8316, pp. 15-18.

6. G. Bertrand and R. Prud'Homme, J. Non-Equilibrium Thermodynamics 4, 1979, 1.

7. H. Wiechert, J. Phys. C9, 1976, 553.

8. U. Schotte and H. D. Denner, Z. Phys. B41, 1981, 139.

9. S. W. K. Yuan et al., Rept. UCLA-ENG-8402, 1984, pp. 3-27.

10. S. W. Van Sciver, Adv Cryog. Eng. 29, 1984,315.

11. G. T. Barnes and D. S. Hunter, J. Colloid and Interface Sci. 88, 1981, 437.

12. R. Evans, Adv. Phys. 18, 1979, 143.

13. R. N. Hills and D. H. Roberts, J. Non-Equilibrium Thermodynamics 4, 1979, 131.

14. W. W. Johnson and M. C. Jones, Adv. Cryog. Eng. 23, 1978, 363.

15. J. T. Tough and M. L. Baehr, Int. Conf. Low Temp. Phys. LT-17, Pt. 1, 1984, 317.

16. T. H. K. Frederking et al., Adv. Cryog. Eng. 19, 1984, 687.

17. J. F. Allen and J. Reekie, Proc. Cambridge Phil. Soc. 35, 1939,

18. W. H. Keesom, Liquid Helium, Elsevier, Amsterdam, 1942.

19. M. Murakami et al., ICEC-9, Proc. 9th Int. Cryog. Eng. Conf., 1982, pp. 184-197.

20. G. Klipping et al., Cryogenics 18, 1978, 166.

21. J. M. Lee, M.Sc. Thesis, Univ. Calif., Los Angeles, 1983.

22. F. A. Staas and A. P. Severijns, Cryogenics 9, 1969, 422.

APPENDIX A

FURTHER DETAILS OF VECTOR QUANTITIES OF THE TWO-FLUID MODEL

Consider the five equations for the superfluid He II density system, for j, for q in terms of the latent heat λ , for q in terms of w , and for w :

$$\rho = \rho_s + \rho_n \tag{A.1}$$

$$\vec{j} = \vec{j}_s + \vec{j}_n \tag{A.2}$$

$$\vec{j} = \vec{q} / \lambda \tag{A.3}$$

$$\vec{q} = \rho_s \vec{w} S T \tag{A.4}$$

$$\vec{w} = \vec{v}_n - \vec{v}_s \tag{A.5}$$

Elimination of v_n to obtain $q(v_s)$. Use of A.4 and A.5 in A.2 with $\vec{v}_n = \vec{w} + \vec{v}_s$ leads to

$$\vec{j} = \rho_n \vec{w} + \rho \vec{v}_s \tag{A.6}$$

Elimination of $\vec{w}$, employing A.4 and A.6 ,yields the desired function:

$$\vec{q} = - \rho \vec{v}_s S T \frac{\rho_s}{\rho_n} \frac{1}{[1 - (\rho_s/\rho_n)(ST/\lambda)]} \tag{A.7}$$

Note : The denominator of (A.7) is always positive in the range of roton excitations, and $\vec{q}$ is opposite to $\vec{v}_s$.

Elimination of v_s to obtain $q(v_n)$. Use of A.1 and A.5 in A.2 with $\vec{v}_s = \vec{v}_n - \vec{w}$ leads to

$$\vec{j} = \rho \vec{v}_n - \rho_s \vec{w} \tag{A.8}$$

The relative velocity w may be eliminated again using the above procedure. The resulting function for q is

$$\vec{q} = \rho \vec{v}_n ST \frac{\lambda}{(\lambda + ST)} \tag{A.9}$$

The factor with the latent heat λ is always positive, and q is in the direction of v_n , as required by the 2nd law of thermodynamics. For illustration, vector examples are shown in Figure A.1

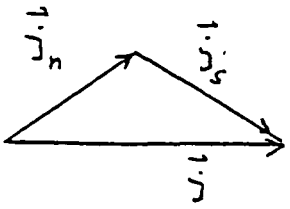

(a) Arbitrary case

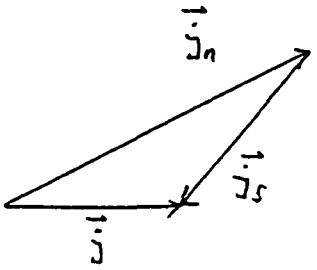

(b) Superfluid velocity component opposite to mass flow component

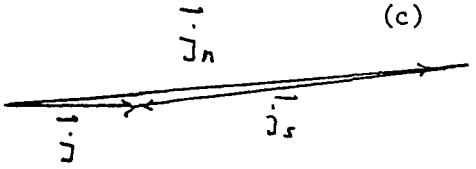

(c) Similar to case (b) with small mass flux density

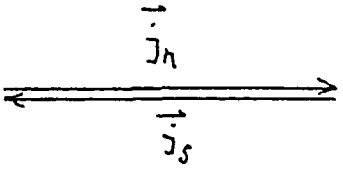

(d) Zero net mass flow

Figure A.1 . Various vectors

APPENDIX B

MEAN TRANSPORT RATES OF THE TWO-FLUID MODEL

Consider mean values of the previous two-fluid equations (e.g. Appendix A). For the phase separator processes, the first law and the second law of thermodynamics requires that j_n and j have a flow direction from the liquid vessel to the vent lines system. , i.e. $|j| + |j_s| = |j_n|$. The preceding equations of Appendix A are re-written as follows:

$$|j| + |j_s| = |j_n| \tag{B.1}$$

$$|j| = |q| / \lambda \tag{B.2}$$

$$|q| = \rho_s |w| S T \tag{B.3}$$

The preceding equation (A.6) of Appendix A becomes

$$|j| + \rho|v_s| = \rho_n |w| \tag{B.4}$$

Elimination of w using (B.3) and (B.4) leads to the function $|q| [|v_s|]$:

$$|q| = \rho |v_s| S T (\rho_s/\rho_n) \frac{1}{\left\{1 - \frac{\rho_s}{\rho_n} ST/\lambda\right\}} \tag{B.5}$$

The mean heat flux density is obtained readily as a function of $|v_n|$ noting that

$$|v_s| = |w| - |v_n| \tag{B.6}$$

Further, the mass flux density is

$$|j| = \rho |v_n| - \rho_s |w| \tag{B.7}$$

The resulting heat flux density is

$$|q| = \rho|v_n|ST \frac{\lambda}{(\lambda + S T)} \tag{B.8}$$

Figure B.1 is an example of the relative velocity $\vec{w}$ in relation to the other velocities of the two-fluid model.

APPENDIX C

TEMPERATURE DIFFERENCE ACROSS THE VAPOR-LIQUID INTERFACE

The temperature difference arising from surface tension of a curved interface is not zero. Consider an interface characterized by a radius of curvature R . The pressure difference associated with a spherical shape is

$$\Delta P = 2 \sigma / R \qquad (C.1)$$

A first order approximation of the related temperature difference is obtained from the Clausius-Clapeyron equation for the vapor pressure. At the low pressures P of the He II- vapor equilibrium the ΔP_v along the vapor pressure curve and ΔT are related by

$$\Delta T = \Delta P_v \; T / (\rho_v \lambda) \; ; \quad \Delta T \ll T \qquad (C.2)$$

After insertion of (C.1) with $\Delta P = \Delta P_v$ into (C.2) we obtain a temperature difference of

$$\Delta T = (2 \sigma / R) \left[T/(\rho_v \lambda) \right] : (\Delta T \ll T) \qquad (C.3)$$

(σ surface tension = 0.33 erg/cm^2 at 2 K). For instance , at 2 K, a radius of curvature of 5 μm gives rise to a temperature difference of approximately 14 milli-K .

APPENDIX D : APPLICATION OF POROUS PLUG FLOW RESULTS FOR FOUNTAIN EFFECT-BASED REFRIGERATION SYSTEM NEAR 2 K

The system including performance figures for a fountain effect refrigerator have been discussed for one particular version, called the He II vortex refrigerator , by the originators Staas and Severijns [22]. The present work has given considerable insight into various operational characteristics associated with fountain effect use in porous plugs. A simplified, ideal cycle is discussed .

Consider the ideal cycle based on the sequence of changes of state as follows : μ - P - μ-P ;(P = pressure; μ = chemical potential). The ideal cycle is shown in Figure D.1 in the lnT-ln S -diagram , and in Figure D.2 in the ln P - T diagram. Ideal heat exchange is presumed, and ideal "superleaks" . It is noted that not all aspects depicted here schematically have been clarified at this time. In particular we remark that the fountain effect in conjunction with the increase of S with a rise in pressure causes peculiarities in cycle operation not known in other refrigeration cycles. Nevertheless, local thermodynamic equilibrium is presumed such that one can draw continuous curves for the changes of state considered.

At point 1 a reference state is attained,e . g. saturated liquid He II. The change of state from 1 to 2 is a compression from P_1 to a higher pressure P_2 . The change of state from 2 to 3 is assumed to be an ideal isobaric heat exchange path . For instance , an aftercooler may operate from T_2 to T_1 during this change of state. If a rather low T is desirable , a counterflow exchanger may be employed for the subsequent lowering of T to T_3 . The change of state from 3 to 4 is ideally at constant chemical potential . This is similar to the ideal pressure increase from 1 to 2 , however at 3 the pressure is being lowered to the initial pressure $P_4 = P_1$.

At point 4 the refrigeration load is taken up by the working substance up to T_3 . If the counterflow heat exchanger is left out , the system is modified, as sketched in Figure D.3 . In this case the refrigeration load is modified to include the temperature range from T_4 to T_1 .

It is noted that power cycle operation is restricted in the amount of work to be gained from an available heat . The volume of the He II changes but little during the cyclic operation. Therefore, a rather small amount of work is extracted from each cycle. In contrast , the FER operation is characterized by a reasonable coefficient of performance once heat exchangers can be compact enough with extended surfaces such that a large area is available for a relatively small volume , e.g. sintered exchangers.

An estimate of the performance is given based on a simplified result for the net work. It is noted from Figure D.4 that the density varies insignificantly with T, and it is primarily a function of the pressure. As the cycle takes place between two pressures , a first order approximation for the net work is $\Delta P \cdot \Delta(1/\rho)$; ρ = density. As we have $\Delta(1/\rho) \approx \Delta\rho/\rho^2$, the net work is about $\Delta P \, \Delta\rho/\rho^2$. The isothermal compressibility K_T is of the order of magnitude 10^{-8} $cm^2/dyne$; ($K_T = \rho \, (\partial \rho / \partial P)_T$) . Thus, we have $\Delta\rho \approx K_T \, \rho \, \Delta P$, and the net work is

$$\oint dW \approx (\Delta P/\rho) \, K_T \, \Delta P = W \qquad (D.1)$$

The refrigeration load of the simple cycle D.3 is $\bar{c}_p \, (T_1 - T_4)$. Consequently, for the simple estimate based on Equation (D.1) we obtain a coefficient of performance of

$$Q_c / W = \bar{c}_p \, (T_1 - T_4) / W \qquad (C.2)$$

For ΔP of the order 0.1 bar , with $\rho \sim 0.1$ g/cm^3 , for $\bar{c}_p$ of the order 1 J/(g K), $(T_1 - T_4)$ of the order of 2 K , one obtains Q /W of the order of 10^4 ; (Kapitza resistance excluded, $W \sim 0.1$ J/kg ; $Q \sim 1$ J/g).

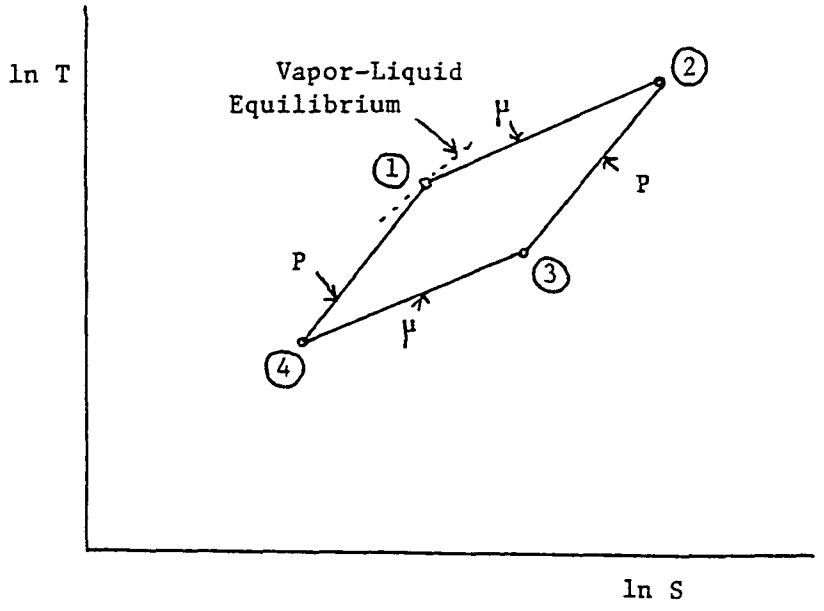

Fig. D.1 . Cycle in the ln T vs ln S diagram, schematically; S entropy

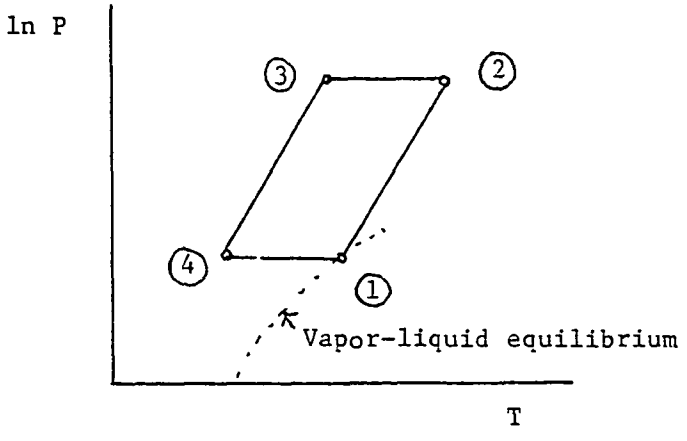

Fig. D.2 Cycle in the ln P vs. T diagram , schematically .

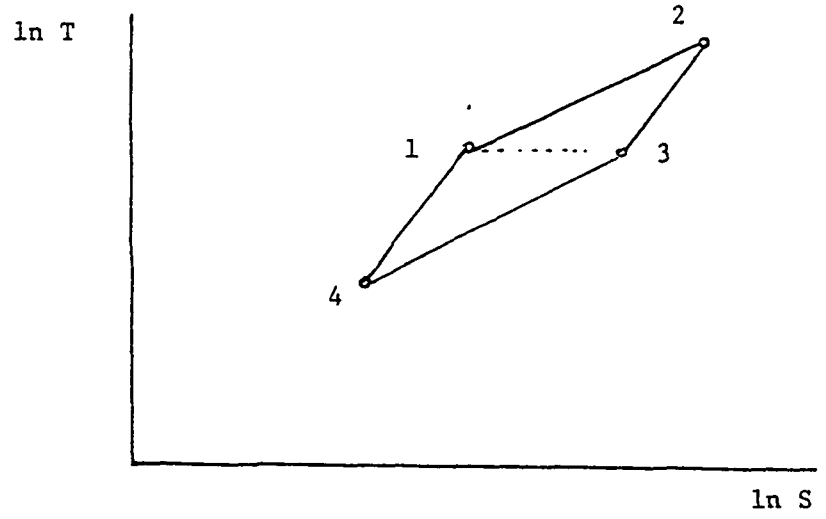

Fig. D.3 . Modified cycle, schematically; $T_1 = T_3$

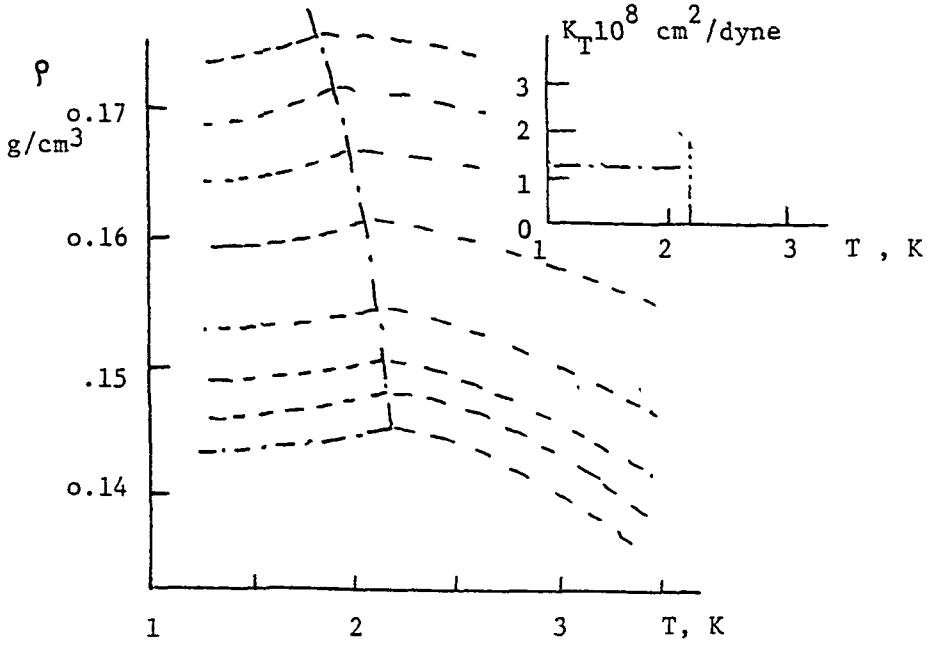

Fig. D.4 . Density vs. T , simplified ; (Inset;: isothermal compressibility)

S U P P L E M E N T I [+]

COMPARISON OF FLOW THROUGH POROUS PLUGS : IS THE DARCY PERMEABILITY A USEFUL MEASURE OF THROUGHPUT ?

J.M. Lee[*], W.A. Hepler, S.W.K. Yuan and T.H.K.Frederking

University of California, Los Angeles , CA 90024 , USA

A B S T R A C T

Size characterization of convective transport through porous plugs in the past appears to have failed to show meaningful lengths generally accepted for the description of throughput in superfluid He II - related applications. It is the purpose of the present studies to obtain the characteristic throughput length L_c (=square root of the Darcy permeability K_D), and to evaluate various phenomena causing departures from Darcy's law. The nominal size range studied extends from the order of magnitude 1 um to 10 um. Data indicate that L_c , in conjunction with the porosity , is a quantity useful for evaluation of the statistical distribution of manufacturing-related plug spectra.

INTRODUCTION

The quantification of flow of cold fluids through porous media has received attention recently in conjunction with vapor liquid phase separation components for liquid He II vessels operating in space /1/ . In the past sintered plugs have been used most frequently for filtration tasks. Parameters pertaining to exterior surfaces of the plugs have been of prime interest. They may depart from interior properties dominating the throughput . The latter ought to be known for optimum liquid retention in the vessel, at minimum liquid He II losses, by means of fountain effect forces.

In general, two-phase conditions have to be addressed. However , single - phase flow appears to be known only to a limited extent for the sintered metal plugs of interest. Recent studies /2/ indicate that the length L_c may be uniquely defined, provided the plugs are clean, and the transport takes place in the Stokes -Darcy regime at small laminar flow speeds. Several parameters may cause departures of the effective permeability (K_{eff}) from K_D . Therefore, the present work is concerned with phenomena disturbing Darcy convection. It is noted that "permeability" in the literature often is used as an operational term. An example is the permeability of diffusive permeation of gas through glass dewar walls, e.g. Dushman /3/. In contrast, the Darcy-value K_D is discussed in the present work. The experiments are outlined, and finally conclusions are drawn concerning the usefulness of K_D .

CONVECTION PERMEABILITY OF SINGLE-PHASE FLOW

In sintered porous plugs, the well-defined conditions of monosized, near-spherical particle assemblies of packed beds are approached

*) Present address: NASA AMES Research Center , Moffett Field, Calif.

+) Presented at Space Cryogenics Workshop, Berlin, Aug. 1983.

only in restricted cases. Nevertheless related equations, such as Ergun's function, have been used as reference . In addition, the simplest geometries may provide ideal permeabilities for infinitely thin walls in the Stokes regime of low speed. According to Darcy's law , the volumetric flow rate, per total cross sectional plug area, ($\bar{v}_o$) is proportional to K_D , to the driving pressure gradient, (grad P), and inversely proportional to the shear viscosity (η) .

$$\bar{v}_o = K_D \, |\text{grad } P| / \eta \qquad (1)$$

For a fluid-filled annulus , with diameters D_o and D_i , the Darcy permeability for very thin walls may be expressed as

$$K_D = D_{eff}^2/32 \qquad (2)$$

with $D_{eff}^2 = (D_o^2 + D_i^2) - (D_o^2 - D_i^2)/\ln(D_o/D_i)$. In the limit of zero inner diameter the tube result ($D_o^2/32$) is recovered , and in the limit of a very narrow slit , the value $(D_o^2-D_i^2)/48$ is obtained.

Among the single-phase phenomena which may perturb the flow are the following conditions: 1. Temperature effects; 2. High-speed phenomena of incompressible fluid flow; 3. Compressible fluid flow effects; 4. Mean free path effects during transition toward Knudsen transport.

Temperature influence. In the present experiments with gas, the mass flow rate has been measured downstream at room temperature $T = T_e$ when the fluid has the density $\rho = \rho_e$. The resulting value of K_D at low speed and $T \neq T_e$ is

$$K_D = (\rho_e/\rho) \, \bar{v}_{o,T_e} \, \eta(T) / |\text{grad } P| \qquad (3)$$

Thus, any T-error caused, for instance by walls at T lower or higher than the fluid temperature results in an effective value K_{eff} smaller or larger than K_D.

High - speed effect. For incompressible fluid, inertia may become significant such that vortex-shedding processes are initiated during the transition into the turbulent flow regime. Ergun's equation /4/ incorporates O.Reynold's linear superposition /5/ of a laminar (Stokes-Darcy) term and a $\bar{v}_o^2$ - contribution to grad P . The resulting effective permeability is

$$K_{eff} = K_D / [\, 1 + \text{Re } 1.75/(150\,\varepsilon^3)^{1/2} \,] \qquad (4)$$

($L_c = K_D^{1/2}$; Reynolds number $\text{Re} = L_c \rho \, \bar{v}_o / \eta$; ε porosity) .

Compressible flow effects. There are limiting boundary conditions of isothermal and adiabatic flow. An approximation for isothermal flow of an ideal gas has been evaluated omitting the Mach number of compressible flow, e.g. /6/ . For large pressure ratios, (P on the upstream side to P on the downstream side), beyond the critical value for a nozzle of about 2, local attainment of the sound speed is probable at the plug exit. The isothermal K_{eff} is known to be above Eq.(4). Thus, the adiabatic K_{eff} is expected to be even larger .As little residence time is available at high speed, the fluid may be close to the adiabatic case.

Knudsen transport influence. When the mean free path starts to become comparable to the pore size of the plug, particle collisions with solids are less frequent than in continuum flow. The resulting |grad P| is smaller for a given flow rate. Thus, K_{eff} becomes larger than K_D .

EXPERIMENTS

Experimental runs with He^4 gas have been conducted with the setup shown schematically in Figure 1. Most of the data have been obtained at room temperature with some extensions to the liquid N_2 boiling point. The gas is admitted from a cylinder, via a pressure reduction valve, to a liquid N_2 trap, transferred into a liquid N_2 - dewar and passed through the porous plug. Mass flow rates are measured downstream. In the course of the work the apparatus, including the thermometry, has been modified. Fluid temperatures are measured upstream and downstream of the plug. Data showing significant T-discrepancies are omitted. Cold fluid data are conveniently taken during slow warmup of the system toward room temperature. Pressure differences are measured with a Validyne P - transducer. Figure 2 presents a data set of K_D versus ΔP in the linear Stokes-Darcy regime at room temperature.

Additional results are obtained readily using flow measurements of Newtonian fluids. Figure 3 shows quasi - steady outflow of liquid from an elevated reservoir through a wire-in-tube system /7/ into an outer bath. In the laminar range, the level difference decays exponentially with time t : $\Delta z/\Delta z_o = \exp(-t/\tau_c)$; τ_c characteristic time. The latter is proportional to the reciprocal permeability, to the length, and the cross sectional area ratio, to the kinematic viscosity, and to g^{-1};(g gravitational acceleration).

Another method is the utilization of "pseudo-classical" flow in the liquid breakthrough mode of vapor -liquid phase separation (Fig.4). He II is kept on the downstream side, however high pressure causes He I conditions on the upstream side /8/. The resulting K_D-values versus the externally applied ΔP are shown in Figure 4.

DATA DISCUSSION AND COMPARISON WITH OTHER RESULTS

The temperature influence on the permeability during He^4 gas flow is displayed in Figure 5 as volumetric flow rate($\dot{V}$) versus ΔP. Low K_{eff}-values are indicated. There is a transition to non-linearity with even lower K_{eff}-results. The insert of Figure 5 shows K_D, low values of K_{eff} caused by low-T walls effects on thermometry, and high K_{eff}-values for "high" -T walls.

Compressible flow effects appear to be involved implicitly in the data of R M German /9/ for stainless steel plugs. Figure 6 displays equivalent Ergun diameters (D_E) as a function of porosity. The Darcy permeability of Ergun's equation is

$$(K_D)_E = D_p^2\ \varepsilon^3\ /[(1-\varepsilon)^2\ 150\ ] \qquad (5)$$

(D_p mean particle diameter of the bed of near-spherical particles). If the sintered plug has similar properties, there should be an equivalent Ergun diameter relatively close to D_p. We obtain from $K_D = L_c^2$:

$$D_E = L_c\ (1-\varepsilon)/\ (\varepsilon^3/150)^{1/2} \qquad (6)$$

The D_E-values at porosities near closely packed spheres appear to vary but little with ε. Thus, in the vicinity of $\varepsilon \approx 1/3$, D_E ought to be a reasonable measure of the sintered particle system. At high and low porosities flow patterns are at variance with the near-spherical, closely packed particle system. It is noted that compressibility affects the high K_{eff}-data / / in Figure 6. Upstream pressures near 4 bar, with downstream pressures near 1 bar, are probably causing local sound speeds. K_{eff} is less likely represent-

ative of Darcy convection once Mach number effects are omitted.

Data are compared readily as long as geometric and flow similarity is maintained. A modified diameter $D_E \varepsilon^{3/2} /(1 - \varepsilon)$ is used . Fig.7 presents this diameter versus L_c . Exact monosphere assemblies ought to be described by a unique point in this diagram. The data spread, for a specified plug, is in part related to tolerances of the manufacturing process. It is seen that various plugs are rea - sonably separated from each other. Figure 8 displays the D_E - distribution of the present plugs with 2 μm limiting pore size , and minimum particle retention respectively (manufacturer quotation). Two plugs of one manufacturer are lower in D_E than the remainder of another manufacturer.

The possibility of Knudsen transport contributions has been checked by measuring the permeability with N_2 gas. For a 2 um plug, K_D has been found to be 10 % larger than the He^4 gas value. This difference,translated into D_E, is small compared to the width of the D_E-distribution in Figure 8.

CONCLUSIONS

From the present results it is concluded that the Darcy permeabil- ity is quite useful for porous media characterization. An equiva- lent diameter may be deduced readily, once K_D and are known. Precautions however are required to avoid disturbing effects.

Concerning low-T methods , we note that several He II-based tech- niques are useful, e.g. transport near the critical Leiden veloc- ity, zero net mass flow and the low-T limit of vapor-liquid phase separation. In addition, the acoustic index of refraction may be potentially useful /9/ .

ACKNOWLEDGEMENTS . The initial phase of this work has been support- ed by NSF , and follow-up work has received partial NASA support (NCC-2-305) . We acknowledge inputs and contributions of Peter Braunstein, Tuan Anh Le and Chau T. Nguyen .

REFERENCSS

1. A.R. Urbach, P.V. Mason, Cryog.Eng.Conf.1983,Colo.Springs, CB-1.
2. T.H.K.Frederking, C. Chuang, Y.Kamioka, J.M.Lee, S.W.K.Yuan,Adv. Cryog. Eng. 29, 687 (1984).
3. S.Dushman, Sci. Foundations of Vacuum Technique, 2nd Ed.,Wiley, New York, 1962, pp. 491 - 500.
4. R.B. Bird, W.E Stewart, E.N. Lightfoot, Transport Phenomena, Wiley, New York 1960, p. 198.
5. O. Reynolds, Papers on Mechan. and Physical Subjects,Vol. 1, Cambridge Univ. Press, Cambridge 1900, pp. 81 - 85.
6. R.M. German , Powder Technology 30, 81 (1981).
7. W.C. Dyckstra, R.C. Amar, T.H.K. Frederking, Adv. Cryog. Eng. 21, 293 (1976).
8. T.H.K. Frederking, A. Elsner, G. Klipping, Adv. Cryog. Eng. 18, 132 (1973).
9. S.Baker, J.Marcus, G.A. Williams,I. Rudnick, Proc. Intern. Sympos on Phys. and Chemistry of Porous Media,AIP Conf. Proc. No.107, 119 (1983).

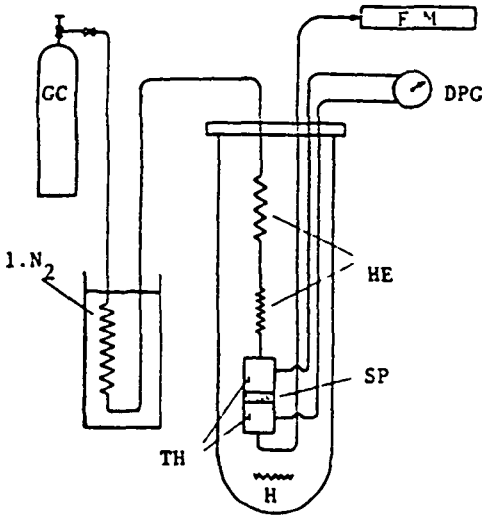

Fig.1. Setup for permeability measurements (schematically); DPG Diff.P-gage;GC gas cylinder FM Flow meter; H heater ; SP Sintered plug; TH thermometers.

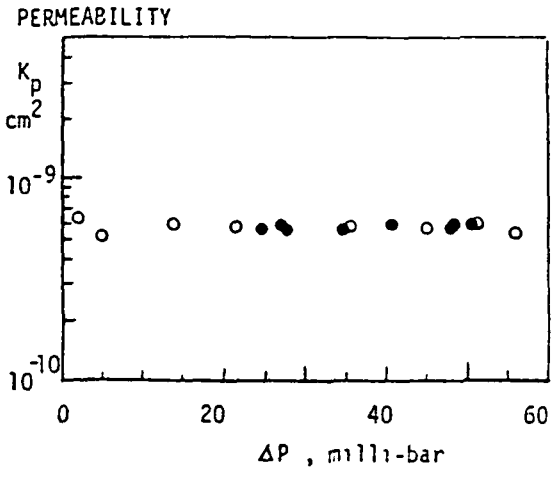

Fig.2. Permeability data at room temperature; He^4 through stainless steel plug (2 μm nominal size); o • two different runs.

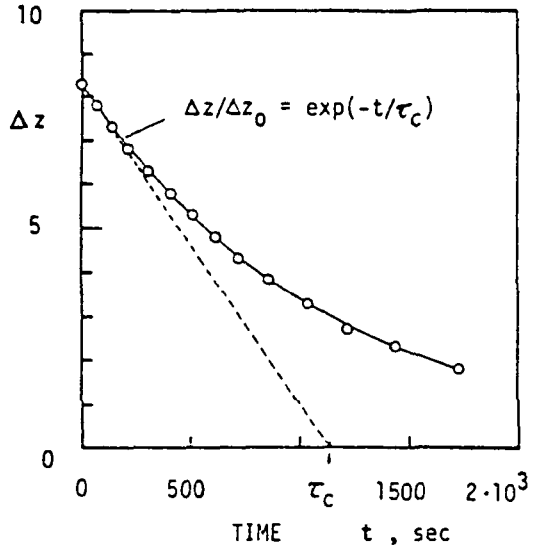

Figure 3. Example of outflow run: Liquid level difference vs t; (liquid N_2 , 1 atm).

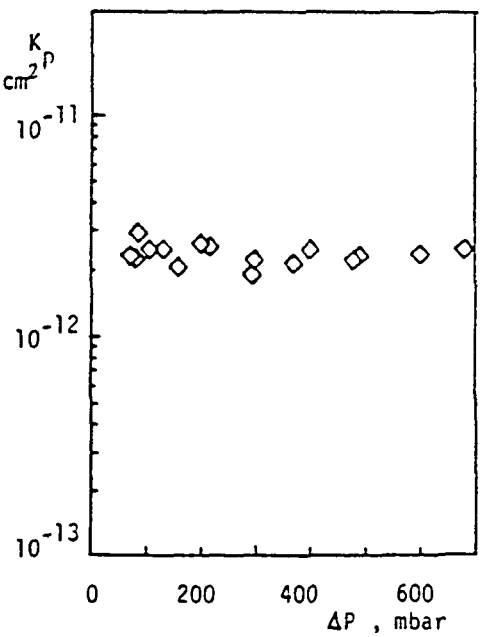

Fig.4. Permeability deduced from breakthrough mode of vapor-liquid phase separation/8/, (nominal size 1 μm;aluminum silicate plug).

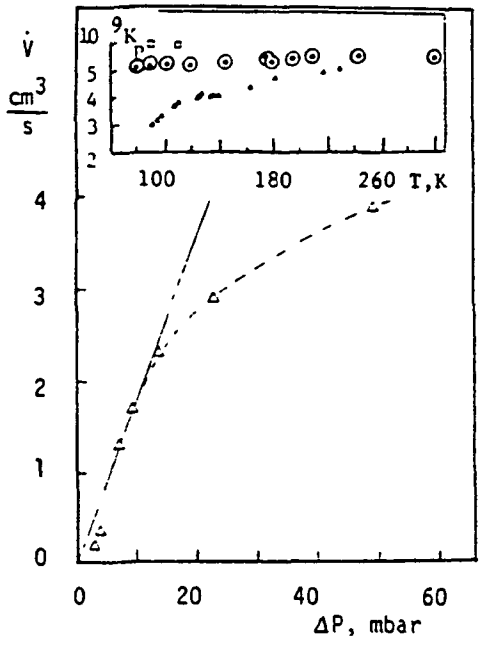

Fig. 5. Volumetric flow rate $\dot{V}$ vs. pressure difference; He^4 at liquid N_2 temperature through stainless steel plug (nominal size 2 μm);
Insert : Permeability vs. T; ($K_p = K_{eff}, cm^2$);
□ "high" T ;
◉ Fluid temperature;
▲ "low" T .

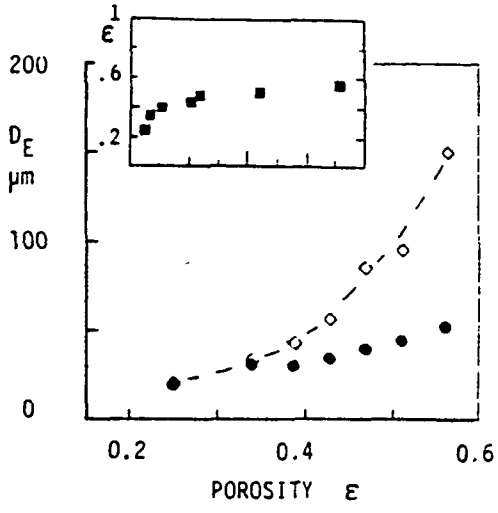

Fig.6. Ergun diameter of equivalent near-spherical particle assembly; (German / 6 /);
Material :Stainless steel;
• Darcy permeability , air;
◇ Data for large ΔP ;
Insert: Porosity vs. mean ■ particle diameter/6/.

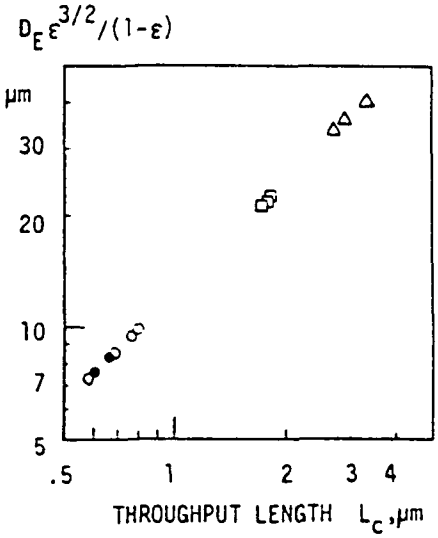

Fig 7. Modified Ergun diameter vs. L_c;
o• Stainless steel plugs 2 μm nominal size;
□ Stainless steel, 10 μm;
△ Bronze plugs (5-15 μm).

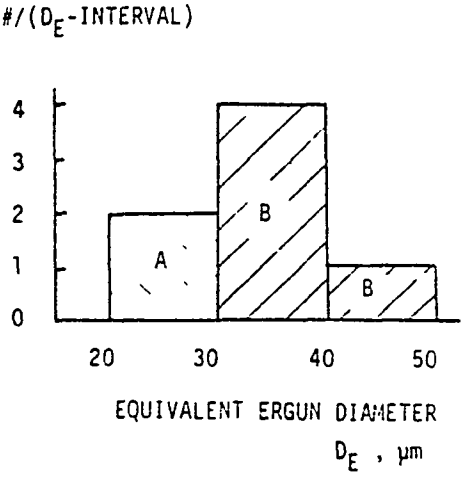

Figure 8. Number of plugs per D_E-interval; (2 μm nominal size, stainless steel).
A Manufacturer "1";
B Manufacturer "2" .

S U P P L E M E N T I I +

THERMODYNAMIC PERFORMANCE EVALUATION OF LIQUID PUMPS BASED ON THE FOUNTAIN EFFECT OF SUPERFLUID LIQUID HELIUM II

S.W. K. Yuan, T.H.K. Frederking and R.M.Carandang

University of California , Los Angeles 90024 CA USA

Thermodynamic performance of thermally activated liquid pumps ("thermopumps") for He II has been evaluated for a heater-activated system("Leiden pump") and a cooler-activated device(Klipping type pump"). The thermopump with a cooler is found to be inferior to the Leiden pump from the point of view of refrigeration power requirements, however it is attractive when cheap refrigeration is available. Transport rates are conveniently based on classical Darcy permeabilities (K_D) when porous plugs are used. Examples are power law approximations for the non - Newtonian flow describing the ratio of the He II permeability K_{II} to K_D. Experiments have been conducted with a Leiden pump fitted with a stainless steel plug characterized by a nominal size of 2 μm .

INTRODUCTION

Recent studies of forced flow of liquid He II , e.g. [1, 2], raise questions concerning the availability of suitable pumps. Several mechanical pumps are potentially useful, e.g. [3, 4], also for He II. However in some cases, pumps without moving parts may give great reliability. These types of pumps are available in the He II temperature range ($T<T_\lambda$ = 2.172 K) on the basis of fountain effect utilization. The pressure difference ΔP_T, generated by a temperature difference, is established across a porous medium. The latter is to suppress backflow of heat and normal fluid of He II toward the low temperature side of the plug. Simultaneously a reasonable throughput of liquid through the pump is to be established. There are two proto - types of thermopumps available: The heater-activated pump is called a Leiden pump because of extensive work at Leiden with this type of pump. The cooler-activated pump, so far, appears to be operated in batch modes for liquid vessel replenishment by Klipping et al. [5] . It is the purpose of the present studies to evaluate thermodynamic work requirements and to assess transport conditions. Experiments have been conducted with a stainless steel pump of the Leiden type.

THERMODYNAMIC EQUILIBRIUM STATE CONSTRAINTS

It is assumed that a near-saturated He II bath is available at the specified temperature T (= initial T-value of the Leiden pump , or final T-value of the Klipping pump). In the limit of a small temperature difference $\Delta T \ll T$, the ideal additional refrigeration energy required per thermal energy of the pump is

$$\Delta E/Q = T_e \, \Delta T \, / \, T^2 \qquad , \quad \Delta T \, / \, T \ll 1 \tag{1}$$

The work is based on the assumption that the environmental temperature (T_e) of about 300 K is the ultimate thermal energy rejection temperature. The pumping conditions are sketched in Figure 1 in the pressure-temperature diagram P(T); (P_v vapor pressure curve). The ideal Klipping pump uses a low ultimate temperature with a small entropy (ρ S) per unit volume ,(ρ liquid density). The fountain pressure difference is

$$\Delta P_T = \int_T^{T+\Delta T} \rho \, S(T) \, dT \tag{2}$$

+) Presented at 10th International Cryog. Engng. Conf. ICEC-10, Helsinki, 1984;(paper 06-5) .

The insert (a) of Figure 1 shows a simple scheme for the Klipping pump, and insert (b) sketches a Leiden pump system with an aftercooler(AC). In the subsequent discussion a specified pressure difference ΔP is assumed in order to compare pump performance quantities. Thus, the pumps in Figure 1 supply the same $\Delta P_T = \Delta P$, and the ultimate pressure is shifted by a constant P-change with respect to the vapor pressure curve $P_v(T)$. The Klipping pump is characterized by a required ΔT_{KP}, and the Leiden pump needs ΔT_{LP}. As the entropy is a monotonically increasing function of T, Equation (1) implies a larger ΔT for the Klipping pump than for the Leiden pump. In the Klipping pump system (insert a), a liquid precooler (PC) is operated by means of a refrigerator (KR). A constant mass flow rate ($\dot{m}$) is supplied from a He II bath (RB) during steady flow of liquid through the porous plug (SP) of the pump. The Leiden pump (insert b) has a heater (H) downstream of the plug (SP). Introducing a power law approximation for the entropy, $S \sim T^{\alpha}$, one obtains thermal energy needed for each thermopump as $Q = \alpha (\Delta P_T / \rho)$. Thus, the ideal thermodynamic work per mass is obtained by insertion of Q into Eq.(1) for $\Delta E/Q$. For an arbitrary ΔT the work per mass of the Klipping pump is obtained as

$$W/m = \alpha \, (\Delta P_T/\rho) \, [(T - \Delta T)^{-1} - T^{-1}] \, T_e \qquad (3)$$

In the related (W/m)-equation for the Leiden pump, a lower numerical value results because of a generally higher temperature. Subsequently, a particular cooler system option is considered for the Klipping pump (insert of Fig. 2). A vacuum pump at an elevated temperature is to exert T-control via vapor pressure control. A mass flow rate m_{KP} is taken from the main bath (RB) to an auxiliary bath (AB) at $(P_v - \Delta P_v)$ whose vapor is pumped off by the vacuum pump (VP). The ideal isothermal work of the vapor removal system is considered for comparison : (R gas constant)

$$W_{KP}/m_{KP} = R \; T_j \, [\ln P_{atm} - \ln(P_v - \Delta P_v)] \qquad (4)$$

Figure 2 presents the work of Equation (4) for various T_j-levels below T_e, i.e. for ideal cold compression of ^4He. In the lower part of Fig. 2 the ideal W/m of Eq. (3) is included. For equal flow rates of steady operation, and at T below 4 K, the effectiveness of the pump, expressed as W_{KP}/W, in the best case does not exceed 10 % significantly near 1.9 K. For cold compression above 20 K, the order of 1 % is reached, and at T_e the pump effectiveness becomes quite small.

TRANSPORT CONDITIONS

The thermopump does not only have to satisfy thermostatic requirements. In addition the mass flux in conjunction with the required plug cross section has to be satisfactory. One may adopt a simplified classification of flow with the following three regimes : 1. Superflow (Landau regime with zero flow resistance);2. Transition regime with vortex shedding processes leading to vortex flow resistance ; 3."Classical" Newtonian fluid flow. Near-critical operation at vortex shedding onset has a small flow resistance. For a tie-in with Darcy convection of Newtonian fluid, the reciprocal resistance ratio is considered a permeability ratio (K_{II}/K_D) for the present studies;(K_D Darcy permeability). In the vortex flow resistance regime the power law approximation of Vote et al. [6] is adopted : For instance, for a sintered 1 μm plug (nominal size), the flow may be described by

$$(K_{II}/K_D) = \zeta_4^{-1} (\rho_s/\rho) [(\rho \, S|\nabla T|) \, \rho \, L_c^{\,3}/\eta_n^{\,2}]^{-3/4} \qquad (5)$$

($L_c = K_D^{1/2}$, η_n normal fluid shear viscosity , $\zeta_4 = 0.56 \pm 0.04$) . The permeability ratio of Eq. (5) is rewritten in terms of the volumetric flow rate per total plug cross section ($\bar{v}_o$) making use of the power law [6] with $\bar{v}_o \sim (\rho \, S \, |\nabla T|)^{1/4}$.

$$(K_{II}/K_D) = \zeta_4^{-4} \, (\rho_s/\rho)^4 \; / \; (\rho \, \bar{v}_o \, L_c / \eta_n)^3 \qquad (6)$$

According to the power law approximation, there is a discrete value of the superfluid transport rate ($\bar{v}_o \, \rho / \rho_s$), multiplied times $L_c^{1/4}$, at the observation limit

for ΔP and ΔT respectively; (Leiden criterion for the superfluid "critical" velocity). At low speed there are departures from the power law, as K_{II} grows beyond all limits at the cessation of the Landau regime. At high speed the vortex shedding processes become disordered and chaotic. Figure 3 shows the permeability ratio, Equation (6), versus the normalized flow rate $(v_o \rho L_c / \eta_n) = (\rho_s v_{os} L_c / \eta_n)$ at several temperatures for the plug of Ref. [6] omitting the vicinity of the lambda temperature . In the frame of Equation (6), flow quantities are affected sensitively by data uncertainty. Therefore, a variation of the constant ζ_4 has been incorporated in the data comparison (caption of Fig.3).

EXPERIMENTS

A small thermopump of the Leiden type has been used for the purpose of replenishment of a liquid jacket simulating a liquid He II vessel during vapor - liquid phase separation experiments [7]. A 2 μm stainless steel plug with a diameter of 1.27 cm and a thickness of 0.3175 cm has been employed with a soldering joint between a surrounding stainless steel tube. The pump is shown schematically in the insert of Figure 4. Satisfactory performance was observed. In line with the experimental procedures used,[7], a drift in temperature was permitted (Fig.4) . In Figure 4 the liquid level z is shown as a function of the time t . In addition the speed $\bar{v}_o \sim dz/dt$ is displayed.

CONCLUSIONS

Thermopumps have advantages when no moving parts are desired for enhanced reliability,when the space required for the pump is not a crucial factor, and when the necessary ΔP-values are not excessive. The effectiveness may be low with some pumping schemes, and the Klipping type pump, at a first glance, appears to be inferior to the Leiden pump. This is not the case however for large scale systems with sufficient refrigeration available at suitable T-levels.

ACKNOWLEDGEMENTS

Part of this work has been supported by Academic Senate (UCLA) Grant 3526. The most valuable inputs of W.A. Hepler and numerical calculations of C. Arboleda are gratefully acknowledged.

REFERENCES

(1) Caspi,S. and Frederking, T.H.K.,'Influence of forced flow on the He II-He I transition in the presence of heat flow, J. Heat Transf.1983, 105, 846-850.
(2) Van Sciver, S.W.,'Heat transport in forced flow He II: Analytic solution', Adv. Cryog. Eng. 184, 29, 315-322.
(3) Swift, W., Sixsmith, H. and Schlafke,A.,'A small centrifugal pump for circulating cryogenic helium', Adv. Cryog. Eng. 1982, 27, 777-784.
(4) Lehmann,W. and Minges, J.,' Operating experience with a high capacity helium pump under supercritical conditions', Adv Cryog. Eng. 1984, 29, 813-820.
(5) Elsner,A. and Klipping, G.,'Temperature and level control in a liquid Helium II cryostat, Adv Cryog. Eng 1973, 18, 317-322.
(6) Frederking,T.H.K., Elsner, A. and Klipping ,G.,' Liquid flow rates of superfluid Helium II during thermomechanical pumping through porous media', Adv Cryog Eng. 1973, 18, 132-140.
(7) Frederking, T.H.K., Chuang,C., Kamioka,Y , Lee.J.M. and Yuan, S.W.K.,'Sintered plug flow modulation of a vapor-liquid phase separator for a Helium II vessel', Adv. Cryog. Eng. 1984, 29, 687-695.

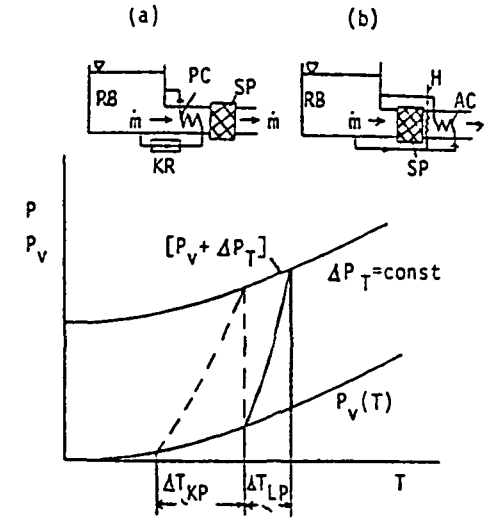

Fig. 1. Pressure-temperature diagram with state changes in thermopumps;
Insert a: Klipping type pump for steady flow of liquid;
Insert b: Leiden pump with heater and aftercooler.

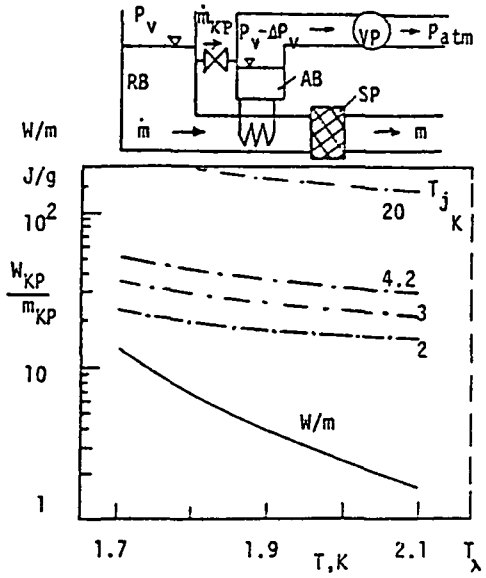

Fig.2. Comparison of energy requirements for ΔP = 100 mbar; $-\cdot-\cdot-W_{KP}/m_{KP}$;
Insert : Example of Klipping type system (schematically) .

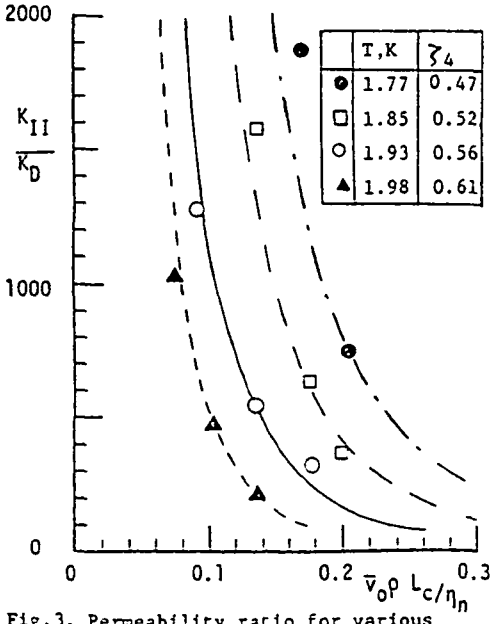

Fig.3. Permeability ratio for various bath temperatures [6] of a 1 µm plug with K_D= 2.5·10^{-12} cm^2 .

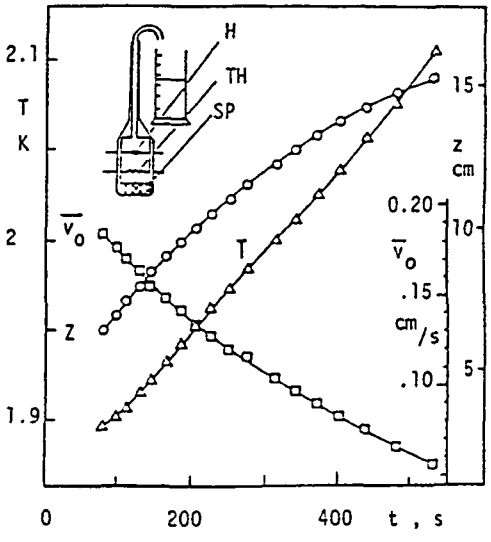

Fig 4. Data of thermopumps experiments versus time ; K_D=3.4 10^{-9} cm^2 at room temperature,
Insert : Pump system, H heater, SP porous plug, TH thermometer; (z liquid level position in vessel) .

S U M M A R Y

This report outlines work performed during Summer 1984 (from June to Sept. 30) in the area of porous media for use in low temperature applications. Recent applications are in the area of vapor - liquid phase separation, pumping based on the fountain effect and related subsystems . Areas of potential applications of the latter are outlined in supplementary work.

Experimental data have been taken to the extent permitted by the limited funding . The linear equations of the two-fluid model are inspected critically in the light of forced convection evidence reported recently. It is emphasized that the Darcy permeability is a unique throughput quantity in the porous media application areas whose use will enable meaningful comparisons of data not only in one lab but also within a group of labs doing porous plug studies.